

# Investigation of the Properties of Nuclear Matter and Particle Structure at the Collider of Relativistic Nuclei and Polarized Protons

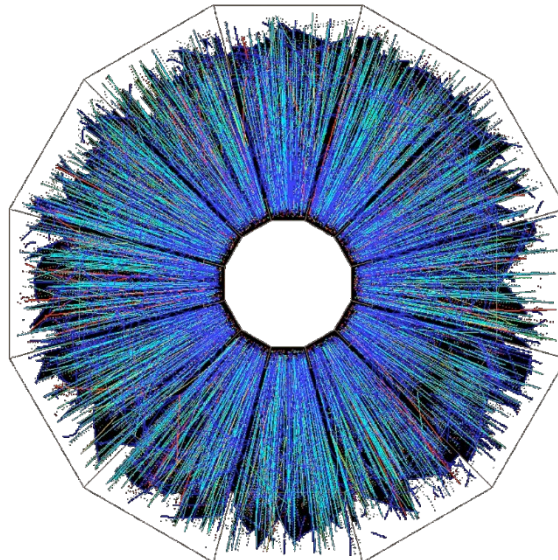
*Project STAR (JINR Participation)*

*Extended annotation*

A. Aitbaev, A.A. Aparin, G.S. Averichev, H.N. Agakishiev, N.A. Balashov,  
T.G. Dedovich, I.Zh. Bunzarov, N.Y. Chankova-Bunzarova, V.B. Dunin, P. Filip,  
A.O. Kechechyan, O. Kenzhegulov, K.V. Klygina, V.V. Korenkov, A.A. Korobitsyn,  
R. Lednický, V.V. Lyuboshitz, S.I. Manukhov, V.V. Mitsyn, M.P. Osmachko,  
G.A. Ososkov, Yu.A. Panebrattsev, S.S. Panyushkina, E.A. Pervyshina,  
E.V. Potrebenikova, N.E. Sidorov, E. Shakhaliyev, S.I. Snigirev, M.V. Tokarev,  
A. Tutebaeva, N.I. Vorontsova, S.F. Vokal, I. Zborovsky

Leaders: Richard Lednický, Yury Panebrattsev

**JINR TOPIC: 02-0-1066-2007/2023**



Dubna, 2021

# Table of Contents

|  |    |
|--|----|
| 1. Introduction .....  | 3  |
| 2. Participation in STAR Project 2019–2021 .....                               | 4  |
| 2.1. Present status of BES-II program measurements .....                       | 4  |
| 2.2. Binding energy for hypertriton and anti-hypertriton .....                 | 6  |
| 2.3. Spectra of charged particles .....  | 7  |
| 2.4. Spin physics results.....   | 8  |
| 2.5. Collective effects for heavy flavor.....                                  | 9  |
| 2.6. Global polarization energy dependence.....                                | 10 |
| 2.7. Cumulative processes in AA collisions .....                               | 12 |
| 2.8. Production of strange particles in $pp$ and AuAu collisions .....         | 13 |
| 2.9. Event-by-Event Fractal Analysis .....                                     | 14 |
| 2.9.1. Fractal analysis of experimental data .....                             | 14 |
| 2.9.2. Monte Carlo study of fractal structure of events .....                  | 14 |
| 2.10. Development of data analysis .....                                       | 16 |
| 2.10.1. Statistical particle identity method .....                             | 16 |
| 2.10.2. Data processing with the Event plane detector .....                    | 17 |
| 2.10.3. Development of particle identification with new detectors set-up ..... | 17 |
| 3. Completion of BES-II Program in 2021.....                                   | 17 |
| 3.1. Collider mode measurements.....   | 17 |
| 3.2. Fixed target experiment at $\sqrt{s_{NN}} = 3.0$ GeV .....                | 18 |
| 3.2.1. High moments of proton multiplicity distributions .....                 | 19 |
| 3.2.2. Hypernuclei production .....  | 20 |
| 3.3. Net-proton kurtosis and light nuclei yield ratio at 16.7 GeV.....         | 21 |
| 4. STAR after BES II.....  | 22 |
| 4.1. Hot QCD Physics (Run-23 & Run-25).....                                    | 24 |
| 4.2. Cold QCD Physics (Run-22 & Run-24) .....                                  | 26 |
| 5. Plans of JINR Group for 2022–2025 .....                                     | 29 |
| 5.1. Femtoscopy Correlation.....   | 30 |
| 5.2. Monte Carlo simulation and software development .....                     | 32 |
| 5.3. Software infrastructure for the STAR data processing at JINR.....         | 34 |
| 6. References .....  | 35 |
| Appendix 1. Form No. 26.....   | 37 |
| Appendix 2. Form No. 29.....   | 38 |
| Appendix 3. List of conference reports .....                                   | 39 |

# 1. Introduction

The goal of the STAR project (JINR participation) is to study the properties of nuclear matter at extreme densities and temperatures, to search for signatures of quark deconfinement and possible phase transitions in heavy ion collisions over a wide energy range at the Relativistic Heavy Ion Collider (RHIC). The research program also includes the study of the structure functions of quarks and gluons in collisions of transversely and longitudinally polarized protons.

In 1993 JINR made a decision on participation of the Laboratory of High Energy and the Laboratory of Particle Physics in the STAR experiment (Solenoidal Tracker at RHIC) at the Relativistic Heavy Ion Collider (RHIC) in Brookhaven National Laboratory. This decision related to extension of the physical research program performed at the Dubna Synchrophasotron to study relativistic hadron-nucleus, nucleus-nucleus interactions and spin physics in collider experiments. The RHIC collider has opened new possibilities to switch to unexplored energy region and study the nuclear matter in extreme conditions.

The experiments with polarized protons were aimed to the direct measurement of the spin-dependent gluon distribution function, determination of the gluon contribution into the proton spin.

Spin is a quantum number characterizing the fundamental property of every particle. It relates to physics symmetries. Therefore, the study of polarization of quarks, gluons and sea quarks in the proton is one of the main problems of the modern particle physics. JINR maintains and develops the tradition of the experimental and theoretical researches in relativistic nuclear physics and spin physics. Note, first of all, the research program with polarized deuteron beams has been successfully performed at the Synchrophasotron. Therefore, the main contribution of the JINR to the STAR project was the participation in the creation of the detectors – the Central Barrel and End Cap Electromagnetic Calorimeters, for the study of the polarization phenomena.

The first run of data taking for Au + Au collisions at STAR has been performed in 2000. After five years of work at maximum RHIC energy main results were formulated: jet quenching, suppression of hadron yields at high transverse momentum, observation of collective flow of nuclear matter, constituent quark number scaling for elliptic flow. Based on the obtained results the important conclusion on creation of the strongly interacting matter in the central nucleus-nucleus collisions has been formulated: the produced matter is similar to perfect liquid and not ideal gas of quarks and gluons. In future the many results observed at RHIC were confirmed at higher energy at LHC.

Even though the experimental program at the STAR facility has been going on for about 20 years, it still remains relevant and brings new striking physical results.

This document is an extended annotation of the Project on JINR's participation in the STAR experiment in the period 2021–2025. This time interval relates to the fact that in the end of 2021 the previous stage of the project ends, the main task of which was data collection and start of data processing using the BES-II energy scanning program. It is important to present the project results obtained by mid-2021 for further planning of the experimental program at the STAR facility and for the participation of the JINR group in it. The end date of 2025 is connected with the fact that for 2022–2025 the STAR collaboration presents a program that is sometimes called STAR after BES-II. In this program, it is planned to extend the acceptance of the STAR facility in the region of forward angles (Mid-rapidity  $-1.5 < \eta < 1.5$  and Forward Rapidity  $2.8 < \eta < 4.2$ ) and in 2022

and 2024 to conduct experiments on the Hot QCD Physics program with beams of gold nuclei at the maximum energy of the RHIC collider. In 2023 and 2025, experiments are planned under the Cold QCD Physics program with transversely polarized protons at an energy of 500 GeV and the collision of polarized protons with nuclei at an energy of 200 GeV, respectively.

The first section of this document is devoted to a discussion of the main physical results and accumulated experimental data in the STAR experiment in 2019–2021, as well as the contribution of the JINR group to this research.

The following sections of the document are devoted to a discussion of the priority physical tasks of the STAR experiment in 2022–2025. First, this is the completion of studies under the BES-II program. There are also two new research programs for 2022–2025 with an expanded acceptance of the STAR facility in the direction of the forward angles – the HOT QCD Physics program in experiments with heavy ions and Cold QCD Physics programs in experiments on the collision of polarized protons and polarized protons with nuclei.

Below the table is showing the request of funding for the project in 2022–2024.

Table 1. Cost Estimate of Project

| № | Name                                  | Full Cost<br>(kUSD) | Expenses per Year (kUSD) |             |             |
|---|---------------------------------------|---------------------|--------------------------|-------------|-------------|
|   |                                       |                     | 2022                     | 2023        | 2024        |
| 1 | Materials and Equipment               | <b>75,0</b>         | 25,0                     | 25,0        | 25,0        |
| 2 | Payments for agreement based research | <b>45,0</b>         | 15,0                     | 15,0        | 15,0        |
| 3 | Travel Expenses                       | <b>165,0</b>        | 55,0                     | 55,0        | 55,0        |
|   | <b>Total direct expenses</b>          | <b>285,0</b>        | <b>95,0</b>              | <b>95,0</b> | <b>95,0</b> |

## 2. Participation in STAR Project 2019–2021

### 2.1. Present status of BES-II program measurements

The most important scientific priority of the STAR collaboration at present time is the energy scanning program – Beam Energy Scan II. The goal of the program is to search for signatures of phase transitions and a critical point of the nuclear matter. The expected result is a significant improvement in our understanding of the phase diagram of nuclear matter. The STAR Collaboration has performed the planned measurements at five collider energies ( $\sqrt{s_{NN}} = 7.7, 9.1, 11.5, 14.6, \text{ and } 19.6$  GeV). In 2021 STAR collaboration is running at minimal RHIC collider beam energy 7.7 GeV (3.85 + 3.85). In Run-21 it is also proposed to additionally carry out measurements at the sixth energy:  $\sqrt{s_{NN}} = 16.7$  GeV. This data will provide a more detailed scan over a range where there are indications that the energy dependence of “net-baryon” fluctuations may be undergoing significant changes (non-monotonic variations in kurtosis  $\times$  variance of the net-proton number distribution as a function of  $\sqrt{s_{NN}}$  with  $3.0\sigma$  significance for central gold-on-gold collisions, Phys. Rev. Lett. **126**(2021)92301).

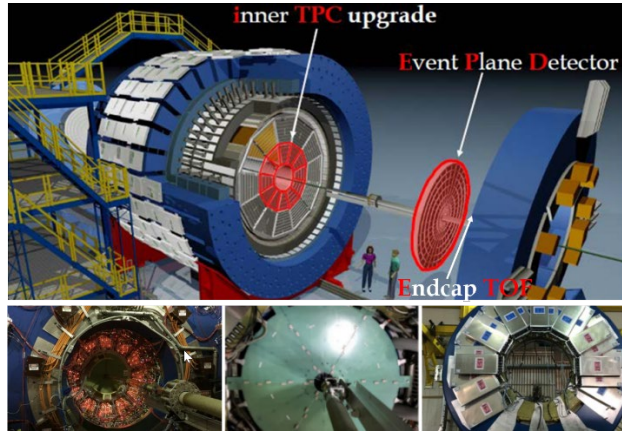


Figure 1. BES II experiments. STAR detector configuration with 3 new detectors (inner TPC, Event Plane Detector, Endcap TOF).

Within the framework of the BES-II research program, a series of experiments on a fixed target was performed. Measurements with a fixed target were also performed, which extend the range of energy scanning to lower energies ( $\sqrt{s_{NN}} = 7.7, 6.2, 5.2, 4.5, 3.94, 3.5$  GeV).

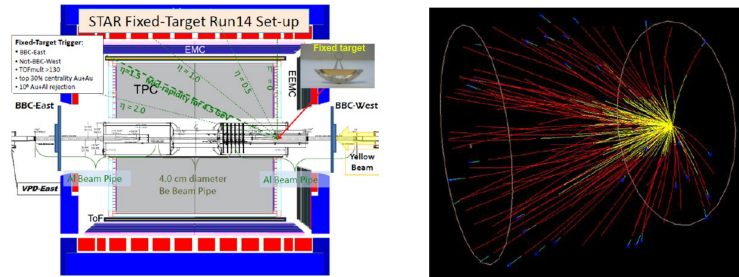


Figure 2. STAR detector configuration for experiments with fixed target.

In the Run-2021, it is planned to additionally collect statistics at the minimum energy in the experiment with a fixed target, which corresponds to the energy of 3 GeV in the center of mass system (the energy in the collider ring – 3.85 GeV).

Below there is a table with the results of measurements performed using the energy scanning program using the BES-II program.

Table 2. Summary of all BES-II and FXT Au + Au beam energies, equivalent chemical potential, requested event statistics, and run times.

| Beam Energy (GeV/nucleon) | $\sqrt{s_{NN}}$ (GeV) | $\mu_B$ (MeV) | Run time  | Number Events |
|---------------------------|-----------------------|---------------|-----------|---------------|
| 9.8                       | 19.6                  | 205           | 4.5 weeks | 400M          |
| 7.3                       | 14.6                  | 260           | 5.5 weeks | 300M          |
| 8.35                      | 16.7                  | 235           | 5 weeks   | 250M          |
| 5.75                      | 11.5                  | 315           | 9.5 weeks | 230M          |
| 4.55                      | 9.1                   | 370           | 9.5 weeks | 160M          |
| 3.85                      | 7.7                   | 420           | 12 weeks  | 100M          |
| 31.2                      | 7.7 (FXT)             | 420           | 2 days    | 100M          |
| 9.8                       | 4.5 (FXT)             | 589           | 2 days    | 100M          |
| 7.3                       | 3.9 (FXT)             | 633           | 2 days    | 100M          |
| 19.5                      | 6.2 (FXT)             | 487           | 2 days    | 100M          |

| Beam Energy (GeV/nucleon) | $\sqrt{s_{NN}}$ (GeV) | $\mu_B$ (MeV) | Run time | Number Events |
|---------------------------|-----------------------|---------------|----------|---------------|
| 13.5                      | 5.2 (FXT)             | 541           | 2 days   | 100M          |
| 5.75                      | 3.5 (FXT)             | 666           | 2 days   | 100M          |
| 4.55                      | 3.2 (FXT)             | 699           | 2 days   | 100M          |
| 3.85                      | 3.0 (FXT)             | 721           | 2 days   | 100M          |

The contribution of JINR group for BES-II run preparation, data tacking and data analysis were:

- Event plane detector assembling and testing;
- distant participation in runs shifts as a shift crew and QA shifters;
- simulation of global polarization and vorticity;
- development of new particle identification algorithms for net baryon fluctuation study;
- JINR GRID Computing.

## 2.2. Binding energy for hypertriton and anti-hypertriton

Among the results that can be attributed to the study of fundamental laws of nature, we note the result of the STAR collaboration on measuring the difference in mass and binding energy of hypertriton and anti-hypertriton (Nature Physics, 16 (2020) 409–412). Nuclear collisions at ultra-relativistic energies, which are studied in experiments at RHIC, produce a hot and dense phase of nuclear matter containing approximately equal amounts of quarks and antiquarks (QGP or Perfect Liquid). In a time of the order of  $10^{-23}$  second this matter passes into a lower-temperature phase containing mesons, baryons, and antibaryons including hypernuclei and anti-hypernuclei. Thus, these collisions provide an ideal laboratory for studying the fundamental properties of interactions involving nuclei, hypernuclei and their antimatter partners. In the STAR experiment in nucleus-nucleus interactions, the first test of CPT – invariance in the sector of hypernuclear matter, where (anti-) strange quarks play an essential role in the formation of these nuclei was carried out. The relative difference in mass between hypertriton and antihypertriton is  $[1.1 \pm 1.0 \text{ (stat.)} \pm 0.5 \text{ (syst.)}] 10^{-4}$ . This indicates the absence of CPT symmetry violations.

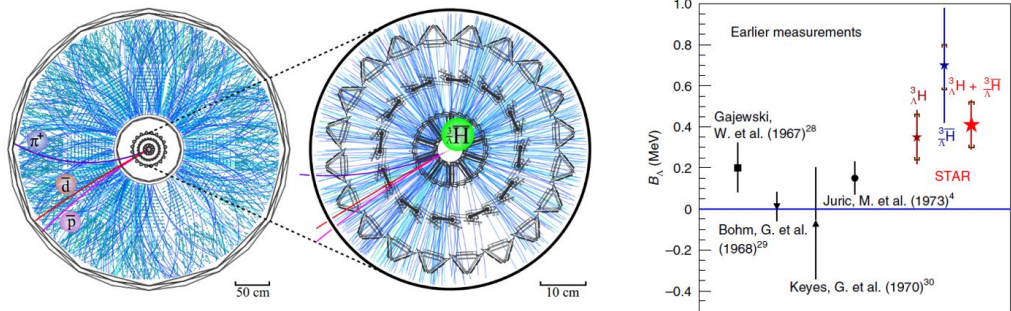


Figure 3. Results on the study of hyperon matter-antimatter ( ${}^3_{\Lambda}\bar{H} - {}^3_{\Lambda}H$ ). Comments to Figure: «Physicists have seen parity violation, and violation of CP together, but no one has looked for CPT violation in the hypertriton and antihypertriton. The previous CPT test of the nucleus was performed by ALICE collaboration (LHC) with a measurement of the mass difference between ordinary helium-3 and antihelium-3. The result shows no significant difference. The STAR results with hypertriton and antihypertriton also reveal no significant mass difference between the matter-antimatter partners explored at RHIC, so there is no evidence of CPT violation».

### Publication:

1. STAR Collaboration, Nature Physics, 16 (2020) 409–412



### 2.3. Spectra of charged particles

As part of the participation in the energy scanning program, a preliminary analysis of the data on the spectra of negatively charged hadrons produced in Au + Au collisions at the energy  $\sqrt{s_{NN}} = 9.2$  GeV and 7.7 GeV (STAR BES-II energy scanning) has been performed. The spectra were studied in a wide range of transverse momentum  $p_T$  and collision centrality (Figure 4). The experimental data were analyzed within the  $z$ -scaling model (Figure 5). The results were presented in the report “High- $p_T$  spectra of  $h^-$  hadrons in Au + Au collision at  $\sqrt{s_{NN}} = 9.2$  GeV” at the STAR collaboration meeting in September 2020 (STAR Collaboration Meeting, September 14–25, 2020).

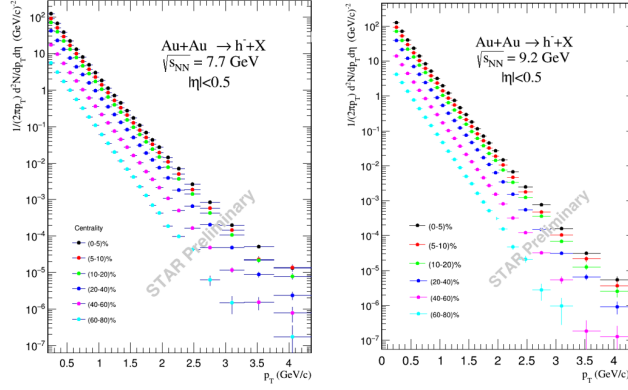


Figure 4. Spectra of negatively charged hadrons versus  $p_T$  for different centralities at collision energy  $\sqrt{s_{NN}} = 9.2$  GeV (energy scan data from BES II).

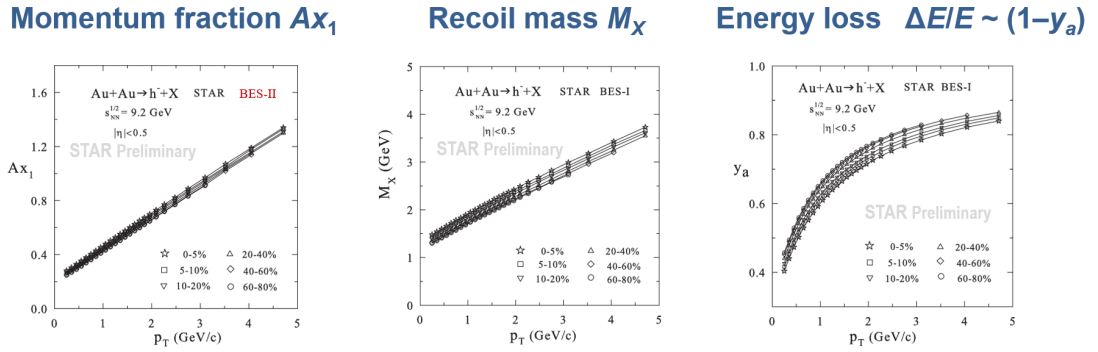


Figure 5. Results of STAR BES-II data analysis at collision energy  $\sqrt{s_{NN}} = 9.2$  GeV within the  $z$ -scaling model (self-similarity of negatively charged hadron production in central Au + Au collision).

The dependence of the momentum fraction, recoil mass and energy loss on transverse momentum of inclusive particles produced in Au + Au collisions at 9.2 GeV and for different centrality shown in Figure 5 demonstrates smooth behavior. The results agree with scaling behavior of the hadron spectra in  $z$ -presentation both in non-cumulative ( $Ax_1 > 1$ ) and cumulative ( $Ax_1 < 1$ ) ranges.

#### **Publications:**

1. A. Kechechyan, M. Tokarev, I. Zborovský  
Nucl. Phys. A993 (2020) 121646 (47 p.).
2. A. Kechechyan, M. Tokarev, I. Zborovský  
Phys. Part. Nucl., 2020, Vol. 51, No. 2, p. 141.
3. M. Tokarev, I. Zborovský  
Phys. Part. Nucl. Let., 2021, Vol. 18, No. 3, p. 302.

## 2.4. Spin physics results

The new results – the double longitudinal asymmetry,  $A_{LL}$ , of pion and jet production at  $\sqrt{s} = 200$  and 510 GeV, the single longitudinal,  $A_L$ , and transverse,  $A_N$ , asymmetry of W production at  $\sqrt{s} = 510$  GeV, are recently obtained by STAR. The growth of the single spin asymmetry  $A_N$  of pion production in experiments with transversally polarized protons was found.

Studying the processes with production of W bosons provides information on the spin-dependent flavor structure of the proton spin. The first measurements of the single longitudinal asymmetry  $A_L$  of  $W^\pm$  boson production in proton-proton collisions at energy  $\sqrt{s} = 510$  GeV allow us to extract spin-dependent distribution of sea  $u$ - and  $d$ -quarks ( $\Delta\bar{u}$ ,  $\Delta\bar{d}$ ). Clear sea  $u$  and  $d$  quark polarization asymmetry is seen based on new STAR data  $\Delta\bar{u} > \Delta\bar{d}$  (see Figure 6).

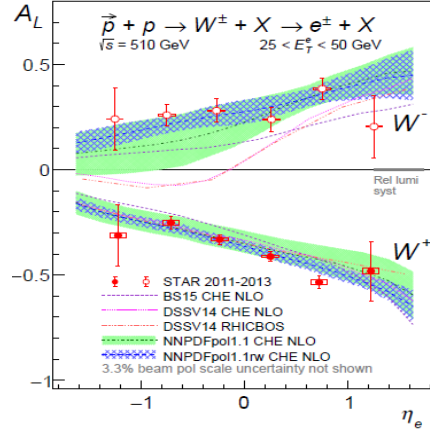


Figure 6. Polarization of the sea quarks ( $\Delta\bar{d} \neq \Delta\bar{u}$ ). Phys. Rev. D 99 (2019) 051102.

The proton consists of quarks and antiquarks, bound by gluons. The gluons provide about half of the momentum of the proton, and their interactions provide most of the mass. Nonetheless, we know very little about the role that gluons play in determining the fundamental proton quantum numbers, such as its spin.

The double longitudinal asymmetry  $A_{LL}$  of the meson and jets production in collisions of polarized protons at the energy of  $\sqrt{s} = 200$  GeV has been measured. The asymmetry was used to extract the spin-dependent gluon distribution. A compelling evidence on positive sign of the integral gluon contribution  $\Delta G$  in the proton spin was obtained (see Figure 8).

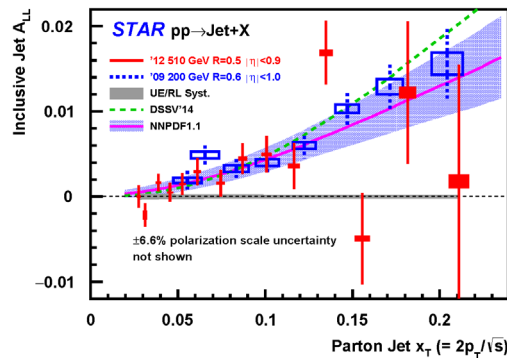


Figure 7. Asymmetry of jet production ( $\Delta G > 0$ ). Phys. Rev. D 100 (2019) 052005.

### Publications:

1. STAR Collaboration, Phys. Rev. D 99 (2019) 051102.
2. STAR Collaboration, Phys. Rev. D 100 (2019) 052005.



## 2.5. Collective effects for heavy flavor

### ▪ *Elliptic flow and Number Constituent Quark Scaling*

The study of nuclear matter in experiments with heavy quarks is one of the main directions of research in the STAR experiment. Elliptic flow is related with collective effects of interacting constituents in nuclear matter.

Elliptic flow  $v_2$  of  $D^0$  mesons in Au + Au collisions at 200 GeV has been measured with the STAR detector using the heavy flavor tracker, a newly installed high-resolutions silicon detector. The measured  $D^0 v_2$  follows the mass ordering at low  $p_T$  observed earlier. The  $v_2/n_q$  of  $D^0$  is consistent with that of other hadrons at  $(m_T - m_0)/n_q < 1$  GeV/ $c^2$  in 10% – 40% centrality collisions. A 3D viscous hydrodynamic model describes the  $D^0 v_2$  for  $p_T < 4$  GeV. Our results suggest that charm quarks exhibit the same strong collective behavior as the light hadrons and may be close to thermal equilibrium in Au + Au collisions at 200 GeV (see Figure 8).

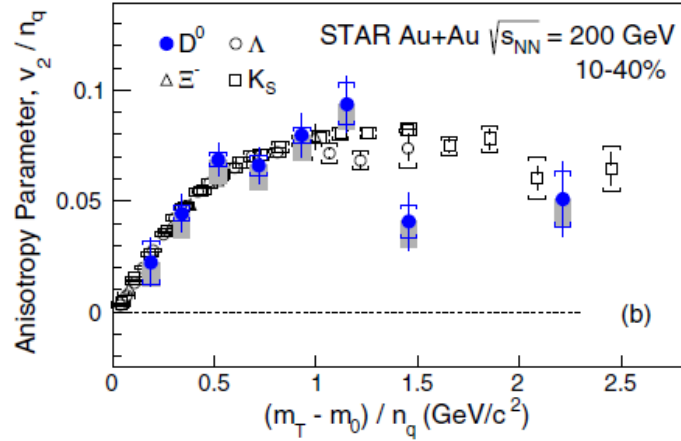


Figure 8. Elliptic flow for heavy quarks ( $D^0$  and other hadrons).

Measurement shows that charm quarks acquire similar elliptic flow as light flavor quarks. This data supposes the strong interaction of charm quarks with QGP.

It was also observed that NCQ scaling is broken at lower energies, where larger  $v_2$  for baryons than antibaryons were observed. Therefore, NCQ scaling for strange and multi-strange hadrons was tested down to  $\sqrt{s_{NN}} = 27$  GeV. The energy scan of  $v_2$  for different at higher  $\sqrt{s_{NN}}$  is also important for search for signature of phase transition and critical point. Elliptic flow is related with collective effects of interacting constituents in nuclear matter.

### ▪ *Nuclear modification factor for heavy flavor*

Over the last few decades, experimental results from RHIC and LHC using light flavor probes have demonstrated that a strongly coupled quark-gluon plasma (sQGP) is created in these heavy-ion collisions. The most significant evidence comes from the strong collective flow and the large high transverse momentum ( $p_T$ ) suppression in central collisions for various observed hadrons including multistrange-quark hadrons  $\phi$  and  $\Omega$ .

Heavy quarks ( $c$ ,  $b$ ) are created predominantly through initial hard scatterings due to their large masses. The modification to their production in transverse momentum due to energy loss and radial flow and in azimuth due to anisotropic flows is sensitive to heavy quark dynamics in the partonic sQGP phase. Transverse mass spectra can be used to study the collectivity of produced hadrons in heavy-ion collisions. Figure 9 shows the  $D^0$  invariant yield at mid-rapidity ( $|y| < 1$ ) as a function of transverse kinetic energy ( $m_T - m_0$ ) for different centrality classes, where  $m_T = \sqrt{p_T^2 + m_0^2}$  and  $m_0$  is the  $D^0$  meson mass at rest.

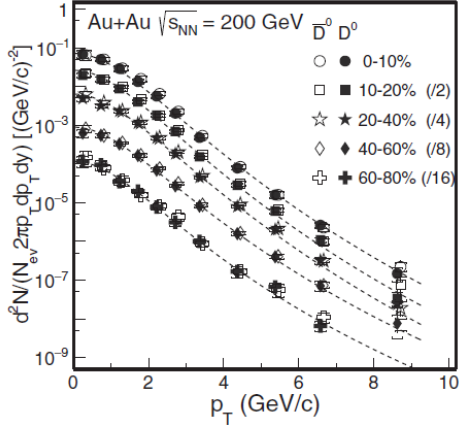


Figure 9. Yields of  $D^0$  mesons produced in Au + Au collisions at  $\sqrt{s_{NN}}=200$  GeV versus transverse momentum for different centrality.

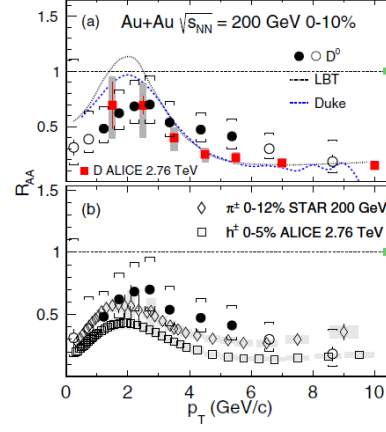


Figure 10. Nuclear modification factor for  $D^0$  mesons produced in central Au + Au collisions at  $\sqrt{s_{NN}} = 200$  GeV versus transverse momentum.

The nuclear modification factors RCP of  $D^0$  mesons is significantly suppressed at high  $p_T$  and the suppression level is comparable to that of light hadrons at  $p_T > 5$  GeV/c (Figure 10). This indicates that charm quarks lose significant energy when traversing through the hot QCD medium.

### **Publications:**

#### 1. STAR Collaboration

“Measurement of  $D^0$  Azimuthal Anisotropy at Midrapidity in Au + Au Collisions at energy 200 GeV”, PRL 118, 212301 (2017)

#### 2. STAR Collaboration

“Centrality and transverse momentum dependence of  $D^0$ -meson production at mid-rapidity in Au + Au collisions at  $\sqrt{s_{NN}}=200$  GeV”, Phys.Rev.C99 (2019) 034908

## **2.6. Global polarization energy dependance**

This first view of the rotational substructure of the fluid at RHIC represents an entirely new direction in hot QCD research. It has generated considerable theoretical activity in the field and may have important connections with the Chiral Magnetic and Chiral Vortical Effects (CME and CVE).

The angular distribution of daughter baryons in the hyperon decays is given by

$$dN/d \cos \theta^* \propto 1 + \alpha_H P_H \cos \theta^*,$$

where  $\alpha_H$  is the hyperon decay constant,  $P_H$  is the hyperon polarization, and  $\theta^*$  is the angle between the momentum of daughter baryon and the polarization vector in the hyperon rest frame. Since the angular momentum of the system is perpendicular to the reaction plane, the polarization of hyperons can be measured via the azimuthal distribution of daughter baryons with respect to the reaction plane in the hyperon rest frame, similarly to anisotropic flow measurements.

Figure 11 presents the global polarization of Lambda and anti-Lambda as a function of the collision energy for the 20–50 % centrality bin in Au + Au collisions. The results from this analysis are shown together with the results from lower collision energies  $\sqrt{s_{NN}} = 7.7–62.4$  GeV. The 2007 result for  $\sqrt{s_{NN}}=200$  GeV has a large uncertainty and is consistent with zero. Our new results for  $\sqrt{s_{NN}}=200$  GeV with significantly improved statistical precision reveal nonzero values of the

polarization signal,  $0.277 \pm 0.040$  (stat)  $\pm 0.039 - 0.049$  (sys) [%] and  $0.240 \pm 0.045$  (stat)  $\pm 0.061 - 0.045$  (sys) [%] for Lambda and anti-Lambda, respectively, and are found to follow the overall trend of the collision energy dependence.

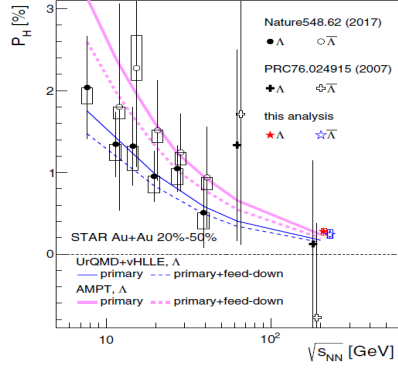


Figure 11. Global polarization of  $\Lambda$  and  $\bar{\Lambda}$  as a function of the collision energy  $\sqrt{s_{NN}}$  for 20–50 % centrality Au + Au collisions.

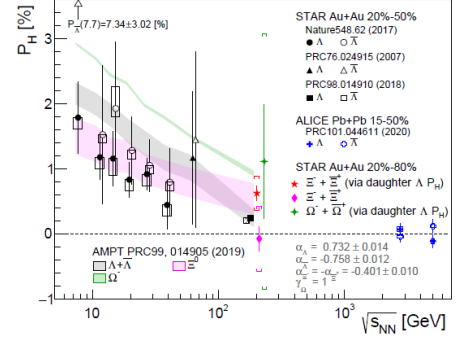


Figure 12. The energy dependence of the hyperon global polarization measurements.

Figure 12 shows new experimental data with the energy dependence of polarization for various hyperons. The figure demonstrates the presence of global polarization in the processes with the birth of not only  $\Lambda$  and  $\bar{\Lambda}$ , but also such particles as  $\Xi$  ( $\bar{\Xi}$ ),  $\Omega$  ( $\bar{\Omega}$ ).

We have also simulated the possibility of studying the global polarization in the energy range of the NICA collider and the acceptance of the MPD detector. As a theoretical model, we used the model “Femto-vortex sheets and hyperon polarization in heavy-ion collisions” (M. Baznat, K. Gudima, A. Sorin, O. Teryaev. Phys. Rev. C93, 031902(2016)). In frame of the model noncentral heavy-ion collisions can generate a rotation with an angular velocity normal to the reaction plane. It is natural to expect that the angular momentum conservation plays an essential role in defining the quantitative properties of vortical effects. The kinetic quark-gluon string model (QGSM) was “Femto-vortex sheets and hyperon polarization in heavy-ion collisions” used to study the time evolution of the angular momentum distribution with considering the contributions from both the participants and spectators. The model was used for Monte Carlo simulation and reconstruction of global polarization of Lambda hyperons produced in Au + Au collisions at NICA energies 5, 7.7, 11.5, 20, 30 GeV. Our results are presented in Figure 13.

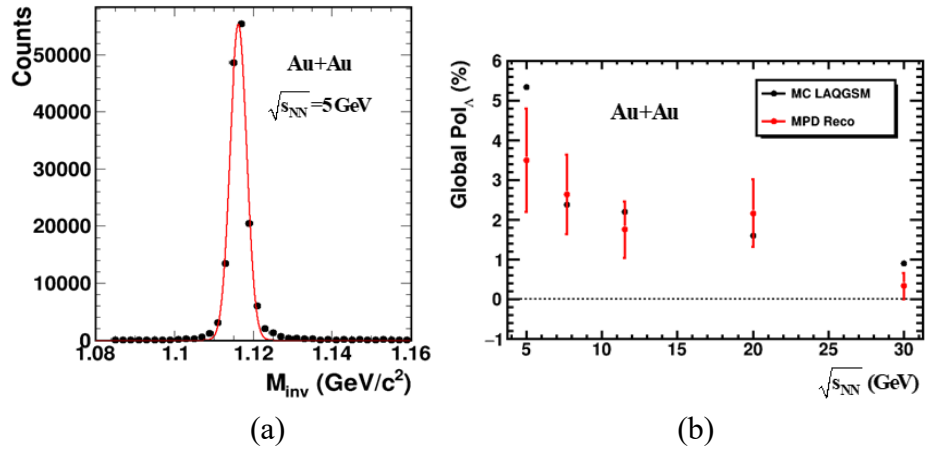


Figure 13. Event distribution on invariant mass ( $p + \pi^-$ ) (a). Global polarization of reconstructed Lambda hyperon versus collision energy  $\sqrt{s_{NN}}$  (b).

**Publications:**

1. STAR Collaboration

“Global  $\Lambda$  hyperon polarization in nuclear collisions”. Nature 548 (2017) 62.

2. STAR Collaboration

“Global polarization of  $X$ ,  $\Xi$  and  $\Omega$  hyperons in Au + Au collisions at  $\sqrt{s_{NN}} = 200$  GeV”. Phys.Rev.Lett. 126 (2021) 16, 162301.

3. STAR Collaboration

“Polarization of  $\Lambda\bar{\Lambda}$  hyperons along the beam direction in Au + Au collisions at  $\sqrt{s_{NN}} = 200$  GeV”. Phys. Rev. Lett. 123 (2019) 13, 132301.

4. STAR Collaboration

“Global and local polarization of  $\Lambda$  hyperons in Au + Au collisions at 200 GeV from STAR”. Nuclear Physics A 982 (2019) 511–514.

**2.7. Cumulative processes in AA collisions**

The high-density nuclear matter can be produced in cumulative processes. Production of any inclusive particle with a momentum far beyond the nucleon-nucleon kinematic region can be accompanied by cumulation of a nucleus. It is assumed that transition of the nuclear matter from the hadron to quark and gluon degrees of freedom near the critical point should reveal large fluctuations, correlations and discontinuity of some experimental quantities characterizing the system. Therefore, particle production in the cumulative regions is of special interest for search for signatures of phase transition and critical point. High sensitivity of elementary constituent interactions to properties of the compressed nuclear matter is expected to be in this region. Study of the cumulative effect is of great interest to search for signatures of phase transitions and a critical point in highly compressed nuclear matter.

The first results on cumulative hadron production in heavy-ion collisions at collider mode are obtained by the STAR collaboration in Au + Au collisions in central rapidity range at  $\sqrt{s_{NN}} = 7.7$  and 11.5 GeV. Results of analysis are shown in Figure 14. The region  $A_{1X_1} > 1$  and/or  $A_{2X_2} > 1$  corresponds to the cumulative processes, indication of which is detection of a cumulative particle. The cumulative particles are particles produced in the kinematic region forbidden for free nucleon nucleon interactions.

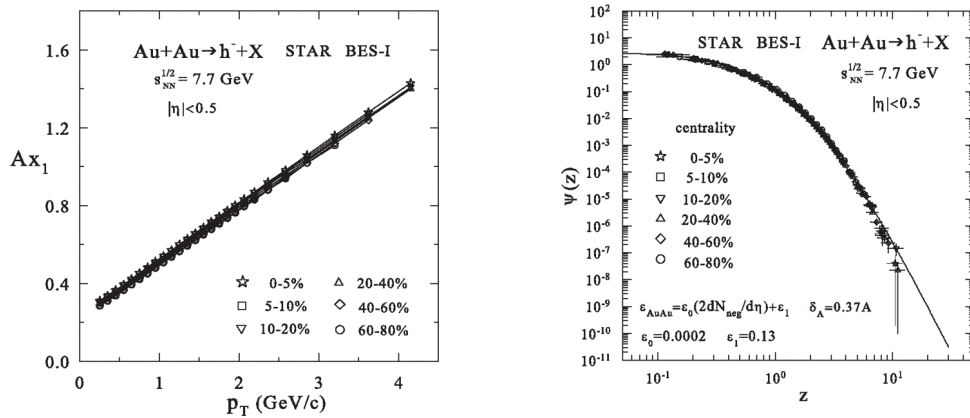


Figure 14. The scaling function  $\psi(z)$  and momentum fraction  $Ax_1$  for negative hadrons produced in Au + Au collisions at the energy  $\sqrt{s_{NN}} = 7.7$  GeV for different centralities. The solid line is a reference curve for  $p + p$  collisions.

**Publications:**

1. A. Kechechyan, M. Tokarev, I. Zborovský

“Validation of  $z$ -scaling for negative particle production in Au + Au collisions from BES-I at STAR”, Nucl. Phys. A993 (2020) 121646 (47 p.).

2. M. Tokarev, A. Kechechyan

“High- $p_T$  spectra of h-hadrons in Au + Au collision at  $\sqrt{s_{NN}} = 9.2$  GeV” STAR Collaboration Meeting, 14–25 September, 2020, Indian Institute of Science Education and Research (IISER) Tirupati, India.

**2.8. Production of strange particles in  $pp$  and AuAu collisions**

Experimental data on transverse momentum spectra of strange particles ( $K_0^S, K^-, K^{*0}, \phi, \Lambda, \Lambda^*, \Sigma^*, \Xi, \Omega$ ) produced in  $pp$  collisions at  $\sqrt{s} = 200$  GeV obtained by the STAR collaborations at RHIC were analyzed in the framework of  $z$ -scaling approach. The concept of the  $z$ -scaling is based on fundamental principles of self-similarity, locality, and fractality of hadron interactions at high energies. General properties of the data  $z$ -presentation are studied. A microscopic scenario of constituent interactions developed within the  $z$ -scaling scheme is used to study the dependence of momentum fractions and recoil mass on the collision energy, transverse momentum and mass of produced inclusive particle, and to estimate the constituent energy loss. We consider that obtained results can be useful in study of strangeness origin, in searching for new physics with strange probes, and can serve for better understanding of fractality of hadron interactions at small scales.

The found feature supports the hypothesis on the universality of the shape of the scaling function for different hadron species ( $K_0^S, K^-, K^{*0}, \phi, \Lambda, \Lambda^*, \Sigma^*, \Xi, \Omega$ ). The observed regularity (the shape of  $\psi(z)$  and its scaling behavior over a wide kinematic range) we treat as a manifestation of the self-similarity of fractal structure of the colliding objects, interaction mechanism of their constituents and processes of fragmentation of the constituents into registered real particles.

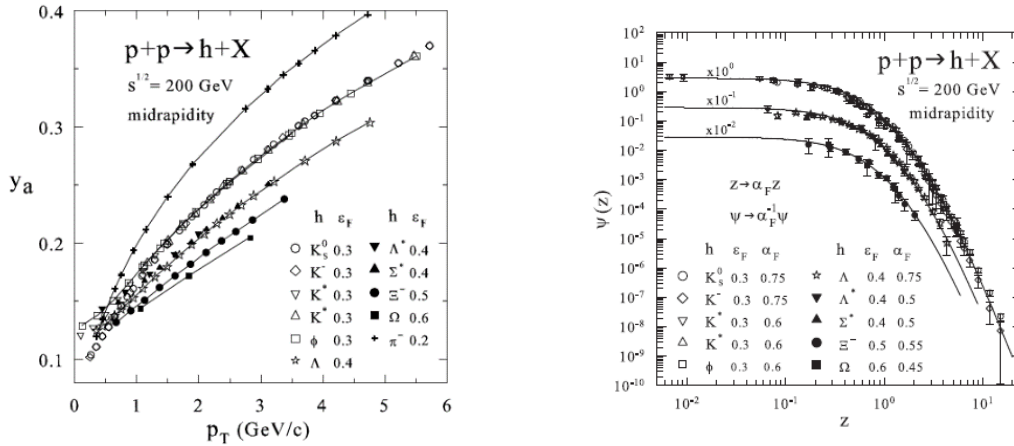


Figure 15. The  $z$ -presentation of the transverse momentum spectra and momentum fraction  $y_a$  of strange hadrons ( $K_0^S, K^-, K^{*0}, \phi, \Lambda, \Lambda^*, \Sigma^*, \Xi, \Omega$ ) produced in  $pp$  collisions at  $\sqrt{s} = 200$  GeV and  $\theta_{cms} = 90^\circ$ .

**Publications:**

1. M.V. Tokarev, I. Zborovskiy, A.O. Kechechyan, T.G. Dedovich

$z$ -Scaling in  $p + p$ , anti- $p + p$  and Au + Au Collisions at RHIC, Tevatron and LHC Physics of Particles and Nuclei, 2020, Vol. 51, No. 2, pp. 141–171.

## 2.9. Event-by-Event Fractal Analysis

### 2.9.1. Fractal analysis of experimental data

The JINR group has developed a method of fractal analysis of events – System of Equations of P-basis Coverage Method (SePaC). The method is based on the property of self-similarity at different levels of resolution in the investigated space (for example, transverse momenta). For each level, the coverage is determined, and an equation is drawn up to find the fractal dimension. The equality of dimensions for all equations of the system determines an object called a fractal. An algorithm for the reconstruction of fractals was developed, the software package was tested on a wide class of fractals, and the effectiveness of the method was estimated (see Phys. Part. Nucl. Lett., 2021, Vol. 18, No. 1, pp. 93–106 and references therein).

A preliminary analysis of the STAR data was performed to search for fractal structures (SePaC-method) in one-dimensional distributions of events in the transverse momentum, pseudo-rapidity and azimuthal angle. The analysis was carried out on statistics about  $10^5$  events in Au + Au interactions at the energy  $\sqrt{s_{NN}} = 200$  GeV. It was found that fractals obtained from the analysis of events in the angle  $\varphi$  have deeper dips in the  $\varphi$  distribution. Fractals and non-fractal events obtained from the analysis of events by pseudo-rapidity differ in the behavior of the  $\eta$ -distribution in the negative region. The behavior of the  $p_T$  spectra of fractals obtained from the analysis of transverse momenta differs from the spectra of non-fractal events in the  $p_T > 2$  GeV region (Figure 16). The distribution of fractals by dimension  $D_F$  has two peaks (two types of fractals). These results were presented in the report “Search for fractal structures in Au + Au events at 200 GeV” at the STAR meeting of the STAR Collaboration Meeting, September 14–25, 2020.

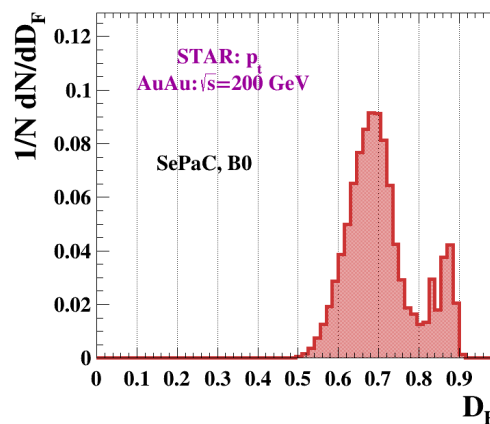


Figure 16. Distribution on the dimension  $D_F$  for fractals obtained by analyzing events by  $p_T$ .

### 2.9.2. Monte Carlo study of fractal structure of events

It is assumed that the SePaC method will make it possible to distinguish events that differ in their transverse momentum distribution. Analyze the selected events considering additional criteria reflecting the mechanism of fractal formation.

The event-by-event analysis of the interactions of nuclei gives the clearest information about the mechanisms of particle formation and the properties of the nuclear medium in a collision, provided that the number of particles in the event is large enough for statistical analysis and the magnitude of the systematic error is comparable to the statistical one.



When describing the mechanism of particle formation in an event, the concept of the formation and development of a shower of quarks and gluons, which evolves and at the final stage of the fragmentation process, turns into observable particles, is widely used. It is assumed that the distribution of particles in the phase space is determined by the dynamics of interaction – the hard interaction of partons, parton shower in the initial and final states, fragmentation of partons into hadrons, and decay of resonances. This scenario is used in many Monte Carlo generators. One of the assumptions of such a scenario is a self-similar shower structure in the space of kinematic parameters ( $\theta$ ,  $Q^2$ ,  $x$  ordering). In each act of parton splitting, the momentum conservation law is fulfilled. Such a self-similar process leads to a fractal distribution of particles in the phase space.

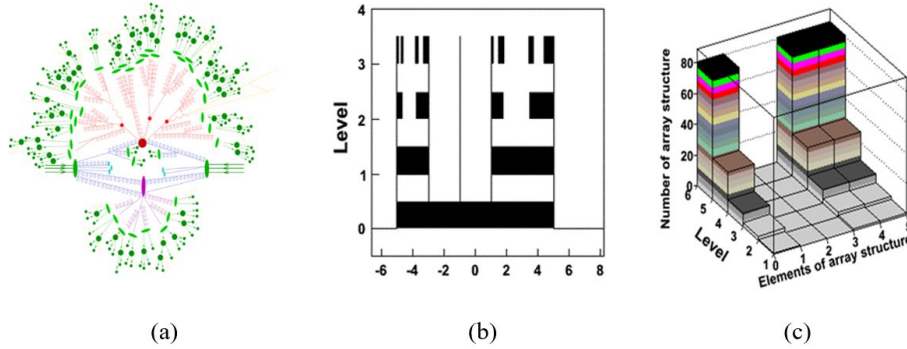


Figure 17. Parton shower (a), Cantor set (b) and its structure (c).

Our work has begun on fractal analysis of STAR data for Au + Au collisions at energy  $\sqrt{s_{NN}} = 200$  GeV. Preliminary results of processing about 1 million events of different centrality were obtained: the optimal parameters of the method were determined, the distributions of events in fractal dimension were obtained, a comparison was made with different  $p_T$ -distributions of particles (power-law, exponential, random), classes of events were identified, the  $p_T$ -distributions of which were differ significantly from each other, additional criteria for selecting events are being developed in order to significantly suppress the background and obtain a cleaner set of fractal events.

The JINR group plans to continue the event-by-event analysis of Au + Au collisions at energies  $\sqrt{s_{NN}} = 200$  GeV and different centralities obtained by STAR at RHIC, with the aim of searching for fractal structures.

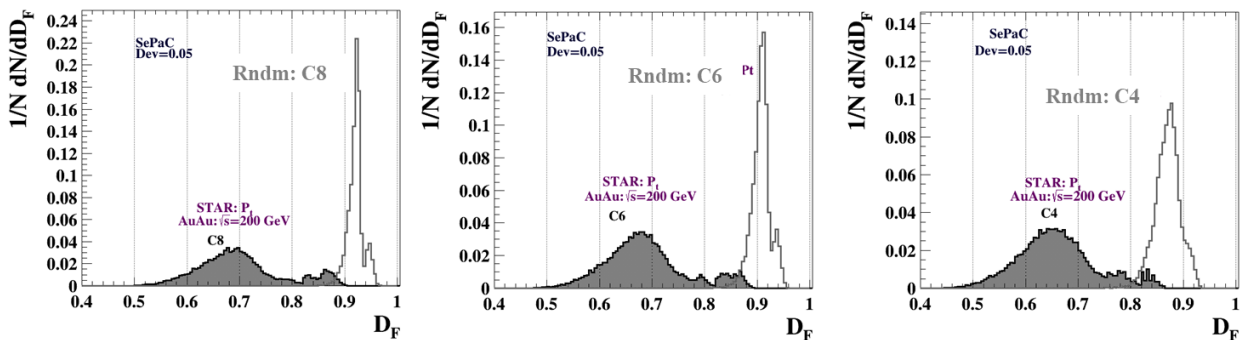


Figure 18. Fractal dimension distribution of Au + Au events (STAR – filled and Monte Carlo (random) – open areas).

**Publications:**

1. T.G. Dedovich, M.V. Tokarev “Incomplete fractal showers and restoration of dimension”, EPJ Web of Conferences 204, 06003 (2019).



2. T.G. Dedovich, M.V.Tokarev

”Reconstruction of the Dimension of Complete and Incomplete Fractals“, Physics of Particles and Nuclei Letters, 16, 3, 240-250, 2019.

3. T.G. Dedovich, M.V.Tokarev

“Criteria of fractal reconstruction and suppression of background events by SePaC method”, Physics of Particles and Nuclei Letters, 2021, Vol. 18, No. 1, pp. 93–106.

## 2.10. Development of data analysis

### 2.10.1. Statistical particle identity method

Transition from hadronic matter to QGP at fixed  $\mu_B$  predicted to be first order. This also mean existence the critical point. Several theoretical models predict irregular behavior of net-baryon density around the critical point. STAR experiment demonstrates the non-monotonic beam energy dependence of ratio of cumulants  $C_4/C_2$  of net-proton multiplicity distribution in AuAu central collisions at BES I energy (Phys. Rev. Lett. **16**(2021)92301).

The value of cumulants is very sensitive to purity of selected events and particles. Published results based on particle identifications by fixed cut on TPC  $dE/dx$  and TOF measurements.

The purity of particle samples can be skewed due to overlaps in  $dE/dx$  and TOF distribution of different spices of particles. Therefore, it will be useful to get same results by different identification methods. We are trying to use for this aim the Statistical Method of PID (identity method) developed in NA49 experiment (Phys. Rev. C83, 054907(2011), Rhys. Rev. C84, 024902(2011)). In this approach one can calculate the particle momentum distributions from TPC  $dE/dx$  response function (see Figure 19).

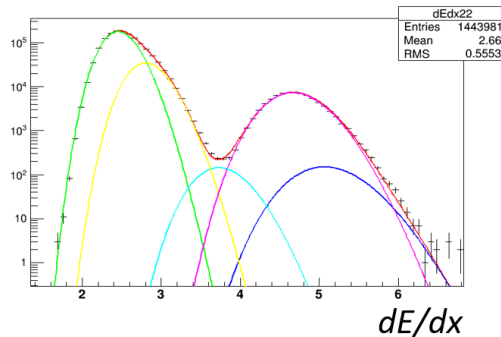


Figure 19. Particle identification TPC  $dE/dx$  response function by statistical (identity) method.

The next pictures (Figure 20) show possibilities of identity method for  $dE/dx$  particle identification.

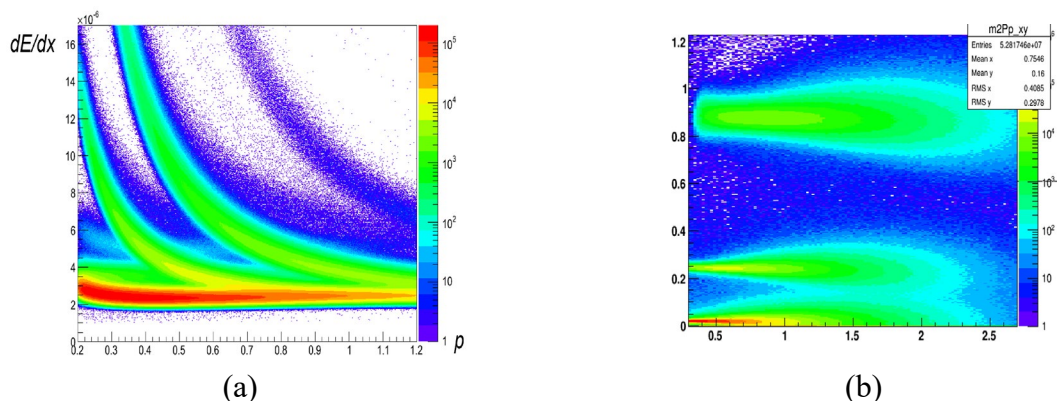


Figure 20.  $dE/dx$  distribution for AuAu 39 GeV (a) and clean sample after identity method (b).

To get detail  $dE/dx$  response functions the high statistics data is needed. We are planning do it using the BES II data collected by collaboration during 2019–2021 years. The software for this analysis is already created and tested at BES I data. These results were presented at STAR Collaboration Meeting, Cracow, 19–23 August, 2019.

### **2.10.2. Data processing with the Event plane detector**

The work related to the inclusion of the event plane detector (EPD) into the complex of programs for data processing. The event plane detector will increase the accuracy of event reconstruction in experiments on studying global polarization and measuring directed flow and other collective effects in nucleus-nucleus collisions. The results of the runs in which the event plane detector worked in the STAR experiment at RHIC since its commissioning in 2018 were analyzed. The software for starting the program code “Event Plane with the STAR EPD code StEpdEpFinder” was installed. Within the framework of StEpdEpFinder, the data on collisions of Au + Au nuclei at the energy  $\sqrt{s_{NN}} = 27$  GeV in the STAR experiment at RHIC, considering information from the event plane detector, have been processed. Using StEpdEpFinder, information about the event plane in collisions of gold nuclei at energies  $\sqrt{s_{NN}} = 27$  GeV was obtained. An estimation was also obtained for the value of the direct flow  $v_1$  for Au + Au collisions at an energy  $\sqrt{s_{NN}} = 27$  GeV. The results of analysis indicate the presence of a nonzero value of  $v_1$ .

### **2.10.3. Development of particle identification with new detectors set-up**

In 2019 and 2020, the STAR collaboration performed a major upgrade of the facility, including new iTPC detector, and collected a large amount of data under the BES II program. Since the increase in the number of points on the track and the new algorithm for calculating the energy losses of particles in the iTPC gas significantly changed the detector response function to different types of charged particles, it became necessary to obtain a new approximation of this function. A significant increase in data statistics and an increase in the efficiency of the software for searching for neutral particles makes it possible to form a new, much cleaner set of particles for determining the response function of both TPCs to protons, pions, kaons and electrons. For this purpose, using the KFParticle algorithm, the distribution of energy losses of different types of particles depending on their momentum and centrality of interaction was obtained from the data processed during the collection of collisions of gold nuclei at different energies. Now, a search is under way for a mathematical function or a set of functions that will allow describing the obtained dependences with an accuracy better than 2 %. Further, these descriptions of the response functions are planned to be applied to determine the magnitude of fluctuations of the moments of the distribution of the multiplicity of particles in collisions of gold nuclei, depending on their centrality and energy.

## **3. Completion of BES-II Program in 2021**

### **3.1. Collider mode measurements**

The highest priority for Run-21 is the completion of the proposed BES-II program. At this time, the only system that remains to be taken is the 7.7 GeV collider data set. This energy is extremely important for several reasons. First, theoretical calculations suggest that the highest baryon density is achieved in collisions at this energy; second, several of the BES-I experimental signatures which have been put forth to be sensitive to the presence of deconfined matter either lose significance or are no longer present at this energy; third, the BES-I data showed enhanced fluctuations at this energy; finally, this energy provides the best acceptance overlap with the fixed-target program. Although the 7.7 GeV collider data set is extremely important from the point of view of the

science, it is also technically the most challenging data set. The technical challenge of achieving a viable collision rate at this energy was the motivation to develop the Low Energy RHIC electron Cooling (LEReC) and is the reason that this energy has been left to the final year of the program.

The specific physics goals (and required statistics) include: measurement of the elliptic flow of the phi meson for which the constituent quark scaling was suggested to break down in the lowest energy BES-I data (80 M events required); measurement of the correlators associated with the charge separation induced by the chiral magnetic effect which were seen to collapse at the lowest BES-I energies (50 M events required); differential measurements of the directed flow of protons which was seen to show evidence of a softening of the equation of state in the lowest BES-I data (20 M events required); Azimuthal femtoscopy measurements of protons to study the tilt angle of the source (35 M events required); measurement of the net-proton kurtosis which showed significant enhanced fluctuations at 7.7 GeV in the BES-I data (70 M events required); measurements of the di-lepton invariant mass distributions to determine in the excess in the low mass region is proportional to the total baryon density (100 M events required); and the global lambda polarization to determine the magnetic field significance (50 M events required). These analyses are being pursued at all of the BES-II collider energies; for several of the physics measurements, the 7.7 GeV energy is expected to be either the most significant or the most challenging.

The 7.7 GeV collider system provides the essential bridge between the collider and fixed-target energy scans. Although in later sections we detail a request to acquire fixed-target data at higher overlap energies, there is the largest region of common coverage at this energy. This will provide critical cross checks between the different modes.

### 3.2. Fixed target experiment at $\sqrt{s_{NN}} = 3.0$ GeV

QCD matter at high baryon chemical potential region contains a wealth of unexplored physics and is one the central focus of current and future heavy-ion collision programs in few GeV energy range around the world. RHIC has been able to deliver beams with the energy as low as 3.85 GeV per nucleon. Utilizing the gold fixed target (FXT) installed in the STAR experiment, we were able to record collision events at the center-of-mass-energy as low as  $\sqrt{s_{NN}} = 3.0$  GeV, which corresponds to baryon chemical potential of  $\mu_B \sim 720$  MeV in central collisions. The STAR detector configuration (including the iTPC and eTOF) has full midrapidity coverage ( $|y| < 0.5$ ) at this energy and enables us to carry a systematic investigation of the dynamics of the QCD matter created in these collisions at  $\sqrt{s_{NN}}$  from 3.0 up to 200 GeV.

At such a high  $\mu_B$  region and moderate temperatures, baryon dynamics become important or even dominant in understanding the QCD matter properties. Strange quarks, due to their heavier masses, play an important role in study the high net-baryon density QCD matter. The combination of increased sensitivity of strange quarks with the existing high baryon density in low energy heavy-ion collisions offers a unique condition to create various light hypernuclei, which enables us to study e.g. the hyperon-nucleon (Y-N) interactions, which have potential implications for the inner structure of compact stars in nuclear astrophysics.

STAR has collected  $\sim 250$  million FXT Au + Au events at  $\sqrt{s_{NN}} = 3.0$  GeV in 2018 before iTPC and eTOF were installed. We propose to collect a minimum of 300 million events with the extended phase-space coverage enabled by iTPC and eTOF for the following measurements:

- high moments of proton multiplicity distributions covering the same midrapidity acceptance

$|y < 0.5|$ ,  $0.4 < p_T < 2.0$  GeV/ $c$ , comparable to that with the BES-I and BES-II measurements in collider mode.

- precision  $\phi$  meson production at midrapidity to test the validity of Canonical Ensemble (CE) for strangeness production at high baryon density region.
- systematic measurements of lifetime, binding energy, production yield, collective flow of light hypernuclei ( ${}^3_{\Lambda}\text{H}$ ,  ${}^4_{\Lambda}\text{H}$ ,  ${}^5_{\Lambda}\text{H}$  etc.).
- measurement of low- and intermediate-mass dileptons to extract fireball lifetime, its average temperature and to access the microscopic properties of matter. This would be the first measurement of electromagnetic radiation at this energy which will guide the future high  $\mu_B$  facilities at FAIR and NICA.

One feature we would like to point out is that the single beam energy for FXT collisions at  $\sqrt{s_{\text{NN}}} = 3.0$  GeV is 3.85 GeV per nucleon, the same beam energy to be used for colliding to collect the major 7.7 GeV collision dataset in Run-21. This leads to a negligible transition time for operation between  $\sqrt{s_{\text{NN}}} = 7.7$  GeV collider mode and  $\sqrt{s_{\text{NN}}} = 3.0$  GeV FXT mode.

### 3.2.1. High moments of proton multiplicity distributions

A non-monotonic behavior of net-proton high moments  $\kappa\sigma^2$  as a function of collision energy has been suggested to be an evidence of the existence of QCD critical point. Figure 21 (left panel) shows the final STAR measurement from the BES-I data as a function of energy exhibiting a suggestive non-monotonic behavior. A complete picture of the non-monotonic behavior requires measurements at collision energies below the lowest collider mode energy (7.7 GeV) by utilizing the FXT mode collisions. STAR detector configuration has the best midrapidity coverage for fixed target collisions at the lowest collision energy  $\sqrt{s_{\text{NN}}} = 3.0$  GeV. Figure 21 middle and right panels show the proton acceptance with TPC and barrel TOF in Run-18 FXT data at 3.0 GeV and Run-10 collider data at 7.7 GeV, respectively. In the 2018 FXT data, to ensure  $> 95\%$  purity of the proton sample, one needs to utilize the barrel TOF for high momentum particle identification. With this requirement, the proton acceptance in Run-18 covers full negative rapidity region ( $-0.5 < y < 0$ ,  $0.4 < p_T < 2.0$  GeV/ $c$ ), while missing a considerable acceptance in the positive rapidity region. A new run, with eTOF and iTPC, would allow for phase space coverage comparable to the one in collider mode (indicated by the box in the middle panel). The estimated acceptance boundary for protons is indicated by the red line shown in Figure 21 middle panel. We can therefore cover the full midrapidity  $y < 0.5$  region from  $0.4 < p_T < 2.0$  GeV/ $c$  which will be the same as these measurements conducted in collider mode data, shown in the right panel. This would allow to perform a systematic scan of the net-proton high moments analysis within the same midrapidity acceptance across the collision energy from 3.0 up to 200 GeV. In the meantime, the increased rapidity coverage will also enable us to investigate the rapidity-window ( $\Delta y$ ) dependence of these fluctuations, which will offer us deep understanding on the physics origin through the development of these fluctuations vs.  $\Delta y$ .

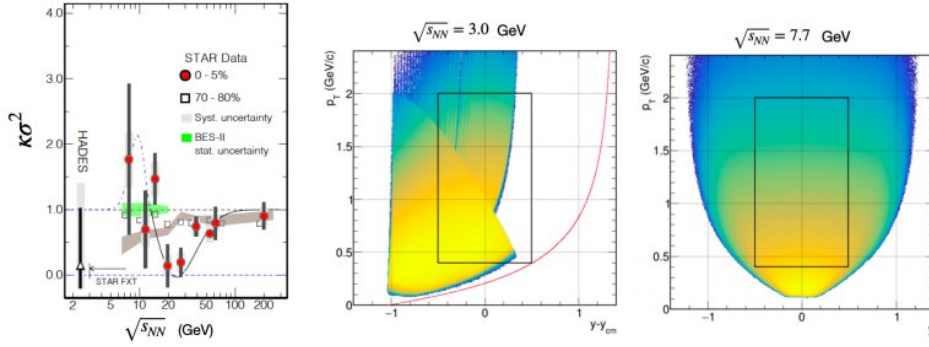


Figure 21. (Left) The net-proton  $\kappa^2$  in most central (0–5 %) and peripheral (70–80 %) Au + Au collisions as a function of collision energy. (Middle/Right) Proton acceptance plot  $p_T$  vs.  $y$  in the center-of-mass frame at  $\sqrt{s_{NN}} = 3.0$  GeV (FXT data from Run-18) and 7.7 GeV (collider data from Run-10), respectively. The red curve in the middle panel indicates the acceptance boundary with iTPC and eTOF.

### 3.2.2. Hypernuclei production

Hypernuclei are those nuclei with one or more nucleons replaced with hyperons (typically  $\Lambda_s$ ). The study of hypernuclei lifetime, binding energy and their production mechanism offer insights to the understanding of hyperon-nucleon (Y–N) interactions. The Y–N interactions could have significant implications to our understanding of the internal structure of compact stars in nuclear astrophysics.

Heavy-ion collisions have shown great potential in studying the light hypernuclei properties and their production mechanism. There have been unprecedented measurements from RHIC and LHC on both the lifetime and binding energy (anti-)hypertriton ( ${}^3_{\Lambda}\text{H}$  and  $\overline{{}^3_{\Lambda}\text{H}}$ ). At low energy heavy-ion collisions, due to the high baryon density and high strangeness population, statistical hadronization thermal model predicts a significant enhancement of various light hypernuclei production yield, shown in Figure 22 left panel. The STAR FXT energy region from  $\sqrt{s_{NN}} = 3.0 - 7.7$  GeV sits nicely in the maximum mid-rapidity production yield of various hypernuclei while STAR detector layout has the best midrapidity acceptance coverage at 3.0 GeV. Figure 22 right panel shows the reconstructed  ${}^4_{\Lambda}\text{H}$  and  ${}^5_{\Lambda}\text{He}$  signal from the Run-18 FXT dataset at  $\sqrt{s_{NN}} = 3.0$  GeV. These are so far the most unprecedented statistics on these light nuclei that will allow us to systematically investigate their lifetimes, binding energies as well as their production yield and collective flow behavior in heavy-ion collisions.

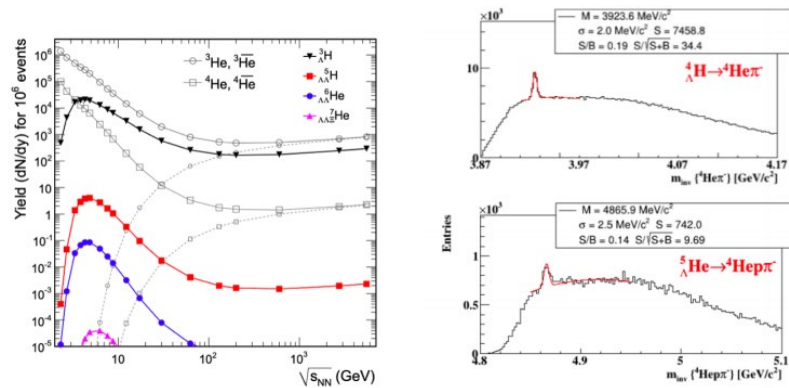


Figure 22. (Left) Thermal model predictions of various light nuclei and hypernuclei production yield at midrapidity in central heavy-ion collisions as a function of collision energy. (Right) Invariant mass distribution of  ${}^4_{\Lambda}\text{He}\pi^-$  (top)  ${}^4_{\Lambda}\text{He}\pi^-$  (bottom) from 2018 FXT data at  $\sqrt{s_{NN}} = 3.0$  GeV. The  ${}^4_{\Lambda}\text{H}$  and  ${}^5_{\Lambda}\text{He}$  hypernuclei signal is clearly visible on top of background.

### 3.3. Net-proton kurtosis and light nuclei yield ratio at 16.7 GeV

The characteristic feature of the Critical Point of the QCD Phase Diagram (CP) is the divergence of the correlation length and density fluctuations. These critical phenomena can be probed by measuring event-by-event fluctuations of conserved quantities, such as baryon, electric charge, and strangeness numbers. The effect of the CP could show as a non-monotonic energy dependence of higher order moments of these conserved quantities in close proximity of the critical point during a beam energy scan.

In the years 2010–2017 RHIC finished the BES-I after taking data in Au + Au collisions at  $\sqrt{s_{NN}} = 7.7, 11.5, 14.5, 19.6, 27, 39, 54.4, 62.4,$  and 200 GeV. With these experimental data STAR measured the higher order fluctuations of net-proton, net-charge, and net-kaon multiplicity distributions. One striking observation was the behavior of the fourth-order cumulants, or kurtosis, of the net-proton fluctuation  $\kappa\sigma^2$  in most central (0–5 %) Au + Au collisions as a function of beam energy. As shown in Figure 23, the fourth order net-proton fluctuation is close to unity above 39 GeV but deviates significantly below unity at 19.6 and 27 GeV, then approaches or turns above unity at lower energies. This behavior may suggest that the created system skims close by the CP and receive positive and/or negative contributions from critical fluctuations.

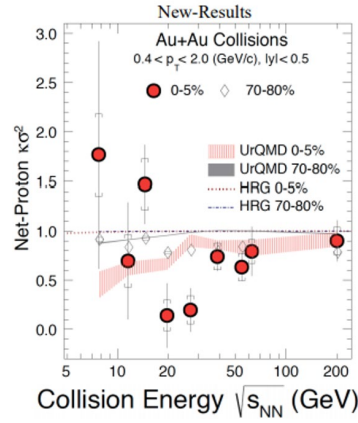


Figure 23. The fourth order net-proton fluctuations  $\kappa\sigma^2$  in most central (0–5 %) Au + Au collisions as a function of collision energy from STAR BES-I measurements.

In addition, STAR has measured light nuclei (deuteron and triton) production in Au + Au collisions at RHIC BES energies. The ratio of these yields is predicted to be sensitive to the neutron relative density fluctuations at kinetic freeze-out, which is expected to increase near the critical point and/or a first order phase transition. The neutron density fluctuation is defined as  $\Delta n = \langle(\delta n)^2\rangle/\langle n\rangle^2$ , which can be approximated from:

$$\Delta n = \frac{1}{g} \frac{N_t \times N_p}{N_d^2} - 1,$$

where  $N_p$ ,  $N_d$  and  $N_t$  are the proton, deuteron and triton yields, respectively and  $g$  is a constant factor of 0.29. In Figure 24, we show the yield ratio  $N_t \times N_p/N_d^2$  in central Au + Au collisions as a function of collision energy. These light nuclei yield ratios are obtained by using the feed-down corrected proton yields, deuteron yield, and preliminary triton results. The ratio as a function of energy exhibits a non-monotonic energy dependence with a peak around 19.6 GeV. The blue band showing a flat energy dependence represents the calculation of the light nuclei yield ratio in Au + Au collisions ( $b < 3$  fm) from a transport JAM model. Furthermore, the yield ratio shown in Figure 24 seems to show a drop between 14.5 and 19.6 GeV.

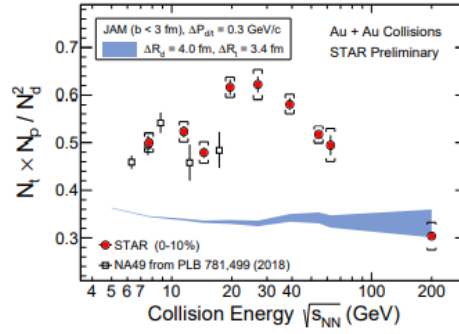


Figure 24. Collision energy dependence of the light nuclei yield ratio ( $N_t \times N_p / N_d^2$ ) in central Au + Au collisions. The open square data based on NA49 results in central Pb + Pb collisions at  $\sqrt{s_{NN}} = 6.3$  (0–7 %), 7.6 (0–7 %), 8.8 (0–7 %), 12.3 (0–7 %), and 17.3 (0–12 %) GeV.

At the end of Run-21, we propose to take one more energy point for Au + Au collisions at 16.7 GeV based on the two observations discussed above and presented in Figure 23 and Figure 24:

1. Net-p kurtosis and light nuclei yield ratio, which are both sensitive to the critical fluctuation, show dip and peak structures around 19.6 GeV. These may suggest that the system passed through the critical region around 19.6 GeV.
2. We observe sudden changes between 19.6 and 14.5 GeV in the energy dependence of net-p kurtosis and light nuclei ratio measurements in the BES-I data measured by the STAR experiment. The neutron density fluctuations at low energies below 14.5 GeV are consistent with the results from NA49 experiment.

These two observations indicate that the critical point may be close to 19.6 GeV. Since there are sudden changes in both observables between 19.6 (chemical freeze-out  $\mu_B = 205$  MeV) and 14.5 GeV ( $\mu_B = 266$  MeV), it is important to conduct a finer beam energy scan between these two energies. Therefore, we request a run with Au + Au collisions at  $\sqrt{s_{NN}} = 16.7$  GeV ( $\mu_B = 235$  MeV), which divides the range into approximately equal  $\mu_B$  gaps.

If nature puts the critical point in the QCD phase diagram between 14.5 and 19.6 GeV (with  $\mu_B$  around 200–270 MeV), RHIC has the best chance to discover it.

## 4. STAR after BES II

In this part of the project the research program of the STAR experiment after BES II period is presented.

At RHIC it is possible to build detectors that can span from mid-rapidity to beam rapidity – with the two recent upgrades STAR is able to achieve this unique capability. STAR’s BES-II upgrade sub-systems comprised of the inner Time Projection Chamber (iTPC,  $1.0 < \eta < 1.5$ ), endcap Time-Of-Flight (eTOF,  $1 < \eta < 1.5$ ) and Event Plane Detector (EPDs,  $2.1 < \eta < 5.1$ ), that are all commissioned and fully operational since the beginning of 2019. The STAR collaboration is constructing a forward rapidity ( $2.5 < \eta < 4$ ) upgrade that will include charged particle tracking and electromagnetic/hadronic calorimetry. For charge particle tracking the aim is to construct a combination of silicon detectors and small strip thin gap chamber detectors. The combination of these two tracking detectors will be referred to as the forward tracking system (FTS). The FTS will be capable of discriminating the hadron charge sign. It should be able to measure transverse momentum of charged particles in the range of  $0.2 < p_T < 2$  GeV/c with 20–30 % momentum



resolution. In what follows, we will refer to the combination of the existing TPC ( $\eta < 1$ ) and the iTPC upgrade as iTPC ( $\eta < 1.5$ ) for simplicity.

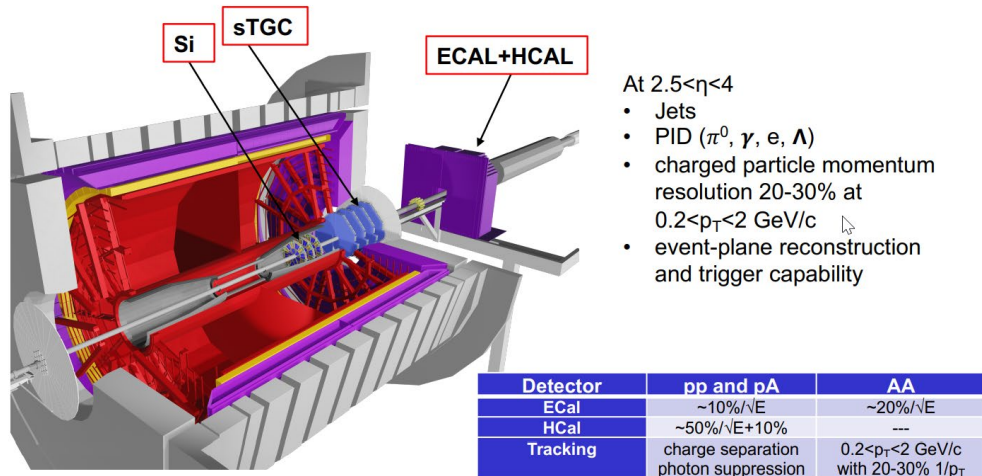


Figure 25. STAR setup further upgrades for experiments after BES II period.

For Run-2022 period STAR Collaboration includes a request for a dedicated 16-weeks  $pp$  run at 500 GeV. This run will take full advantage of STAR’s new forward detection capabilities and further capitalize on the recent BES-II detector upgrades. We motivate a program that will use RHIC’s unique ability to provide transverse and longitudinally polarized proton beams to exploit both an increased statistical power and kinematic reach from recent and planned detector upgrades.

For time period years 2022–2025 STAR collaboration suggests the research program for Mid-rapidity  $-1.5 < \eta < 1.5$  and Forward rapidity  $2.8 < \eta < 4.2$ .

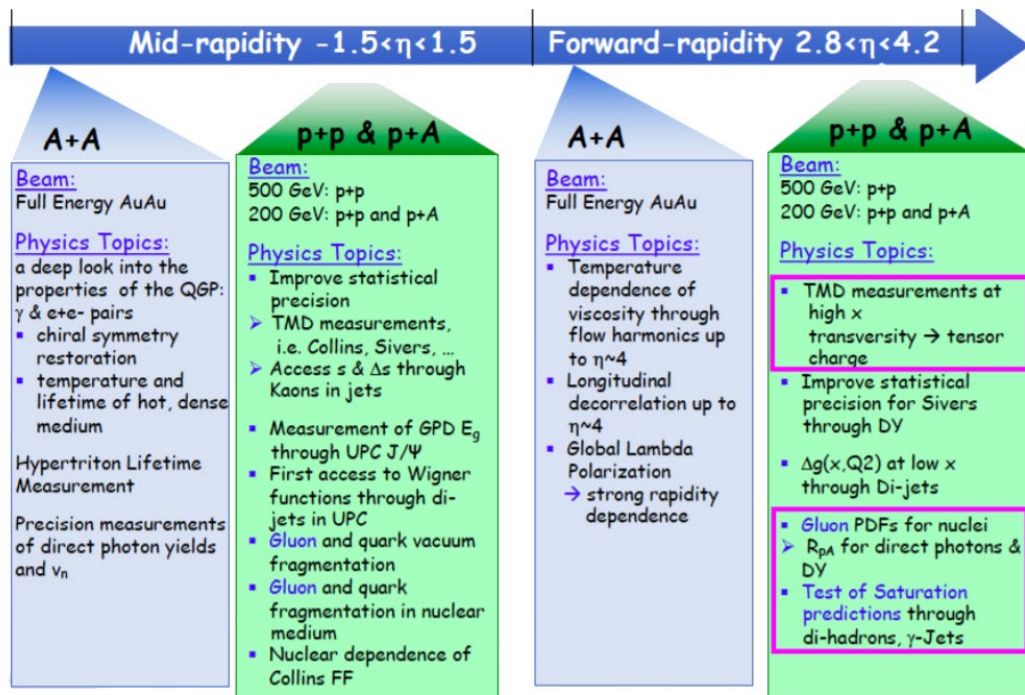


Figure 26. Physics program for mid- and forward rapidities.

For realization of this research program suggested following data tacking runs schedule for years 2022–2025.

## 4.1. Hot QCD Physics (Run-23 & Run-25)

The completion of the RHIC's scientific mission involves the two central goals:

- mapping out the phase diagram of the QCD,
- probing the inner workings of the QGP by resolving its properties at short length scales.

The complementarity of the RHIC and LHC facilities to study the latter is scientifically as essential as having more than one experiment independently study the microstructure of the QGP. With several years of operating the recently installed iTPC upgrade and the soon-to-be installation and operation of STAR's forward detectors, the STAR collaboration will be in an excellent position to take advantage of its vastly improved detection capabilities. Combine this with the prospect of a substantial increase in beam luminosities and RHIC will be uniquely positioned to fully engage in a detailed exploration of the QGP's microstructure. Through careful discussions in its physics working groups, the STAR collaboration has identified a number of topics that together make a compelling case to take data during Runs 23–25 alongside sPHENIX, and successfully complete RHIC's scientific mission. In this section, we present a selection of those topics that will take full advantage of both STAR and RHIC's unique capabilities and address the following important questions about the inner workings of the QGP:

- What is the precise temperature dependence of the shear  $\eta/s$ , and bulk  $\zeta/s$  viscosity?
- What is the nature of the 3-dimensional initial state at RHIC energies? How does a twist of the event shape break longitudinal boost invariance and decorrelate the direction of an event plane?
- How is global vorticity transferred to the spin angular momentum of particles on such short time scales? And how can the global polarization of hyperons be reconciled with the spin alignment of vector mesons?
- What is the precise nature of the transition near  $\mu_B = 0$ , and where does the sign- change of the susceptibility ratio  $\chi_6^B/\chi_2^B$  take place?
- What is the electrical conductivity, and what are the chiral properties of the medium?
- What can we learn about confinement and thermalization in a QGP from charmonium measurements?
- What are the underlying mechanisms of jet quenching at RHIC energies?
- What do jet probes tell us about the microscopic structure of the QGP as a function of resolution scale?

The event statistics projections that are used in this section will rely on the CAD's recently update 2023 and 2025 Au + Au luminosities and are listed in Table 3. For each year we presume 24 weeks of RHIC operations and based on past run operations an overall average of 85 %  $\times$  60 % (STAR  $\times$  RHIC) uptime, respectively. The minimum-bias rates assume a conservative 1.5 kHz DAQ rates which will allow sufficient bandwidth for specialized triggers which are listed as integral luminosities. To achieve the projected luminosities, the collaboration will look into optimizing the interaction rates at STAR by allocating low and high luminosities periods within fills.

Table 3. STAR minimum bias event statistics and high- $p_T$  luminosity projections for the 2023 and 2025 Au + Au runs. For comparison the 2014/2016 event statistics and luminosities are listed as well.

| year | minimum bias<br>[ $\times 10^9$ events] | high- $p_T$ int. luminosity [ $\text{nb}^{-1}$ ] |                      |                      |
|------|---|--|----------------------|----------------------|
|      |   | all vz   | $ vz  < 70\text{cm}$ | $ vz  < 30\text{cm}$ |
| 2014 | 2                                       | 26.5   | 19.1                 | 15.7                 |
| 2016 |   |  |                      |                      |
| 2023 | 10                                      | 43   | 38                   | 32                   |
| 2025 | 10                                      | 58   | 52                   | 43                   |

The impetus for running STAR during the year of 2023–2025 in terms of bulk correlation measurements in Au + Au 200 GeV collisions comes from gains via: extended acceptance and enhanced statistics.

Next, thanks to a reduced material budget between the beam and the iTPC, STAR will be uniquely positioned to perform dielectron measurements with which we propose to probe degrees of freedom of the medium and its transport properties. For that we will use the high precision dilepton excess yield, i.e.  $l^+l^-$  invariant mass distribution after subtraction of dilepton sources produced after freeze-out, and contributions from the initial collisions such as Drell-Yan and correlated charm-anticharm pairs. Furthermore, we propose to study the virtuality, Wigner function and final-state magnetic field in the QGP. For the latter photon-photon collisions in ultra-peripheral, peripheral, and midcentral reactions and  $p + A$  (all centralities) in both channels  $e^+e^-$ ,  $\mu^+\mu^-$  will be measured with high accuracy.

▪ ***Pseudorapidity dependence of global hyperon polarization***

One of the key sets of measurements is of interests – pseudorapidity dependence of global hyperon polarization.

The global polarization of hyperons produced in Au + Au collisions has been observed by STAR. The origin of such a phenomenon has hitherto been not fully understood. Several outstanding questions remain. How exactly is the global vorticity dynamically transferred to the fluid-like medium on the rapid time scales of collisions? Then, how does the local thermal vorticity of the fluid gets transferred to the spin angular momentum of the produced particles during the process of hadronization and decay? In order to address these questions, one may consider measurement of the polarization of different particles that are produced in different spatial parts of the system, or at different times. A concrete proposal is to: 1) measure the  $\Lambda$ (anti- $\Lambda$ ) polarization as a function of pseudorapidity and 2) measure it for different particles such as  $\Omega$  and  $\Xi$ . Both are limited by the current acceptance and statistics available. With the addition of the iTPC and FTS, and with high statistics data from Run-23 it will be possible to perform such measurements with a reasonable significance. iTPC (+ TPC) has excellent PID capability to measure all these hyperons. Although the FTS has no PID capability we can do combinatorial reconstruction of  $\Lambda$ (anti- $\Lambda$ ) candidates via displaced vertices. A similar analysis was performed and published by STAR using the previous FTPC. In order to make a conservative projection we assume similar momentum resolution of 10–20% for single charged tracks, similar overall tracking efficiency, charge state identification capability for the FTS and FTPC (see the forward upgrade section for exact numbers). We also assume the FTS, with its novel-tracking framework, will be able to measure a minimum separation of 20 cm between the all pairs of one positive and one negative track (a possible decay vertex) from the main vertex of the event. This will give rise to about 5 % efficiency

of  $\Lambda$ (anti- $\Lambda$ ) reconstruction with about (15–20) % background contribution from  $K_S^0 \rightarrow \pi^+ + \pi^-$ . With this we can make projections for a polarization measurement in Au + Au 200 GeV (40–80) % assuming 10 Billion minimum-bias events. Currently theoretical models predict contradictory trends for the pseudorapidity dependence of  $\Lambda$  polarization. If the initial local orbital angular momentum driven by collision geometry plays a dominant role it will lead to increases of polarization with pseudorapidity. On the other hand, if the local thermal vorticity and hydrodynamic evolution play a dominant role it will predict decreasing trend or weak dependence with pseudorapidity. Such tensions can be easily resolved with the future proposed measurement during Run-23.

## 4.2. Cold QCD Physics (Run-22 & Run-24)

The exploration of the fundamental structure of strongly interacting matter has always thrived on the complementarity of lepton scattering and purely hadronic probes. As the community eagerly anticipates the future Electron Ion Collider, an outstanding scientific opportunity remains to complete “must-do” measurements in  $p + p$  and  $p + A$  physics during the final years of RHIC. Much of the Run-22 and Run-24 physics program outlined here is, on the one hand, unique to proton-proton and proton-nucleus collisions and offers discovery potential on its own. On the hand, these studies will lay the groundwork for the EIC, both scientifically and in terms of refining the experimental requirements of the physics program, and thus are the natural next steps on the path to the EIC. When combined with data from the EIC these STAR results will provide a broad foundation to a deeper understanding of fundamental QCD.

Beginning in Run-22, STAR will be in a unique position to provide this essential  $p + p$  and  $p + A$  data. A full suite of forward detectors will be installed, providing excellent charged particle tracking at high pseudorapidity ( $2.5 < \eta < 4$ ) for the first time, coupled with both electromagnetic and hadronic calorimetry. This will enable STAR to explore the interesting regimes of high- $x$  (largely valence quark) and low- $x$  (primarily gluon) partonic physics with unparalleled precision. In addition, mid-rapidity detector upgrades motivated primarily by the BES-II program – the iTPC, eTOF, and EPD systems – will substantially extend STAR’s already excellent kinematic reach and particle identification capabilities beyond those that existed during previous  $p + p$  and  $p + A$  runs.

In Run-22 at 510 GeV and Run-24 at 200 GeV the combination of 510 GeV  $p + p$  collisions and the STAR Forward Upgrade will provide access to forward jet physics at perturbative scales, thereby enabling measurements at the highest and lowest  $x$  values. The mid-rapidity measurements at 510 and, especially at 200 GeV will interpolate between the high and low- $x$  values, with significant overlaps to probe evolution effects and provide cross-checks. Together, the two runs will allow STAR to measure fundamental proton properties, such as the Sivers and transversity distributions, over nearly the entire range  $0.005 < x < 0.5$ .

Run-24 will also provide outstanding opportunities to probe fundamental questions regarding QCD in cold nuclear matter. The STAR Forward Upgrade will enable an extensive suite of measurements probing the quark-gluon structure of heavy nuclei and the regime of low- $x$  non-linear gluon dynamics. STAR will also explore how a nucleus, serving as a color filter, modifies the propagation, attenuation, and gluons.

STAR requests in Run-22 at least 16 weeks of polarized  $p + p$  data-taking at  $\sqrt{s} = 510$  GeV involving transversely polarized beams focus on those observables where factorization, universality, and/or evolution remain open questions, with spins aligned either vertically or

radially at the STAR. Assuming we will have running conditions similar to those achieved in Run-17, we expect to sample at least  $400 \text{ pb}^{-1}$  for our rare /non-prescaled triggers.

In Run-24 STAR also requests at least 11 weeks of polarized  $p + p$  data-taking at  $\sqrt{s} = 200 \text{ GeV}$  and 11 weeks of polarized  $p + \text{Au}$  data-taking at  $\sqrt{s_{NN}} = 200 \text{ GeV}$ . All of the running will involve transversely polarized protons, with the choice between vertical or radial polarization to be determined during the coming year. We expect to sample at least  $235 \text{ pb}^{-1}$  of  $p + p$  collisions and  $1.3 \text{ pb}^{-1}$  of  $p + \text{Au}$  collisions.

In experiments with polarized protons, it is supposed to carry out the following measurements.

- ***Inclusive transverse spin asymmetries at forward rapidities***

Transverse single-spin asymmetry  $A_N$  measurement at forward rapidity for hadrons will be studied at highest RHIC energy 510 GeV as a function  $x_F$ . Verification of possible mechanisms of experimental observed TSSA allows to understand the role of transverse-momentum-dependent (TMD) parton distribution and fragmentation functions and independence of the asymmetry on center-of-mass energy. The  $A_N$  data for charged hadrons provide new constraint for evolution and flavor dependence of the twist-3 ETQS distributions.

- ***Transversity, Collins Function and Interference Fragmentation Function***

The  $p\uparrow + p$  collisions is an ideal tool to explore the fundamental QCD questions of TMD factorization, universality, and evolution.

Measurements at  $\sqrt{s} = 200$  and  $510 \text{ GeV}$  will provide additional experimental constraints on evolution effects and provide insights into the size and nature of TMD observables.

Transversity as well as longitudinally distributions of partons in proton are needed for complete understanding nucleon spin structure. The transversity distribution described the transverse polarization of quarks within a transversely polarized proton. Both distributions for quarks and anti-quarks are connected to nonzero orbital angular momentum components in the wave function of the proton. Transversity distribution can also shed light on the tensor charge distribution – new fundamental quantity of the spin structure of the nucleon. The  $k_T$  integrated quark transversity distribution can be extracted from the single spin asymmetry  $A_N$  of the azimuthal distribution of hadrons in high energy jets. The collinear transversity distribution couples to the TMD Collins function and therefore it is possible to directly probe the Collins fragmentation function. The transversity distribution can also be extracted from the single spin asymmetry of pion pairs through the collinear interference fragmentation function.

The fragmentation of linearly polarized gluons into unpolarized hadrons is an equivalent for the Collins fragmentation function. The linear polarization of gluons is an unexplored phenomenon. The measurement of “Collins-like” asymmetries is an important example to access the distribution of linearly polarized gluons. The best kinematic region to access this distribution is at backward angles with respect to the polarized proton and at small jet  $p_T$ .

- ***Sivers and Efremov-Teryaev-Qiu-Sterman Function***

Both the Sivers and the ETQS functions encapsulate partonic spin correlations within the proton, but they are formally defined in different frameworks. The Sivers function is a TMD quantity that depends explicitly on spin-dependent transverse partonic motion  $k_T$ , the ETQS function is a twist-3 collinear distribution, in which Single Spin Asymmetry are generated through soft collinear gluon radiation.

The Sivers effect manifests itself as a correlation (a triple product) between the transverse momentum of a parton ( $\vec{k}_T$ ) with momentum fraction  $x$ , and the transverse spin ( $\vec{S}$ ) of a polarized proton moving in the longitudinal ( $\vec{p}$ ) direction. Thus, for transversely polarized protons, the Sivers effect probes whether the  $k_T$  of the constituent quarks is preferentially oriented in a direction perpendicular to both the proton momentum and its spin.

Runs with transversally polarized  $p + p$  and  $p + Au$  collisions at  $\sqrt{s_{NN}} = 200$  GeV (spin/cold QCD run) will provide STAR with the unique opportunity to investigate these collision systems with the Forward Upgrade providing full tracking and calorimetry coverage over the region  $2.5 < \eta < 4$  and the iTPC providing enhanced particle identification and expanded pseudorapidity coverage at mid-rapidity. These powerful detection capabilities will enable critical measurements to probe universality and factorization in transverse spin phenomena and nuclear PDFs and fragmentation functions, as well as low- $x$  non-linear gluon dynamics characteristic of the onset of saturation. The mid-rapidity  $p + p$  measurements at 510 and, especially at 200 GeV, will interpolate between the high and low- $x$  values, with significant overlaps to probe evolution effects and provide cross-checks. These runs will allow STAR to measure fundamental proton properties, such as the Sivers and transversity distributions, over nearly the entire range  $0.005 < x < 0.5$  and clarify the role of Efremov-Teryaev-Qiu-Sterman function in formation of single spin asymmetry  $A_N$ .

- ***Polarized  $p\uparrow + p$  and  $p\uparrow + A$  collisions at 200 GeV***

Run with transversally polarized  $p + p$  and  $p + Au$  collisions at  $\sqrt{s_{NN}} = 200$  GeV will provide STAR with the unique opportunity to investigate these 200 GeV collision systems with the Forward Upgrade.

- ***Forward transverse spin asymmetries***

The forward transverse spin asymmetries in  $p + p$ ,  $p + Al$ , and  $p + Au$  collisions vs.  $x_F$  and  $p_T$  contains information on the dynamics that underlie the large asymmetries both in  $p + p$  and  $p + A$  collisions. The asymmetry is substantially larger for isolated  $\pi^0$  than when it is accompanied by additional nearby photons. The observed nuclear dependence is very weak. The STAR will enable measurements of  $A_N$  for  $h^{+/-}$ , in addition to  $\pi^0$ , with isolation criteria for nearby charged, as well as neutral, fragments. It will enable full jet asymmetry and Collins's effect measurements.

- ***Sivers effect***

The measurements of dijet production in  $p + p$  are crucial to explore questions regarding factorization of the Sivers function. In Run-24 the data will reduce the uncertainties for  $|\eta_3 + \eta_4|$  and will provide a detailed mapping vs.  $x$  for comparison to results for Sivers functions extracted from SIDIS, Drell-Yan, and vector boson production.

- ***Transversity and related quantities***

Measurements of the Collins asymmetry and IFF in  $p + p$  collisions at RHIC probe fundamental questions regarding TMD factorization, universality, and evolution. The observed asymmetries are functions of jet ( $p_T, \eta$ ), hadron ( $z, j_T$ ), and  $Q^2$ . Measurements in Run-22 at high- $x$  with the Forward Upgrade and at low- $x$  with the STAR mid-rapidity detectors will provide a significant overlapping region of  $x$  coverage. The high statistical precision of the Run-24 data will enable detailed multi-dimensional binning for the Collins asymmetry results and provide a direct probe of the Collins fragmentation function. The asymmetry  $A_{UT}$  vs.  $p_T$  provides information about the transversity distribution.

STAR at RHIC has the unique opportunity to extend the Collins effect measurements to nuclei and verify the universality of the Collins effect in hadro-production by dramatically increasing the color flow that can break factorization for TMD PDFs like the Sivers effect. This will also explore the spin dependence of the hadronization process in cold nuclear matter.

## 5. Plans of JINR Group for 2022–2025

Based on the tasks formulated in the project, we propose the following schedule for the JINR group (see Table 4).

Table 4. Schedule of the project

| No. | Activity  | Years |      |      |      |      |
|-----|---|-------|------|------|------|------|
|     |   | 2021  | 2022 | 2023 | 2024 | 2025 |
| 1   | BES II Data Tacking Run   |       |      |      |      |      |
| 2   | BES II Data Analysis  |       |      |      |      |      |
| 3   | Cold QCD Physics with $p\uparrow + p\uparrow$ Collisions at 510 GeV               |       |      |      |      |      |
| 4   | Cold QCD Physics with $p\uparrow + A$ Collisions at 200 GeV                       |       |      |      |      |      |
| 5   | Hot QCD Physics   |       |      |      |      |      |
| 6   | Study of Femtoscopy Correlation, Event Structure, Global Polarization, High $p_T$ |       |      |      |      |      |

Below in this chapter is a list of tasks that are of particular interest to the JINR group:

1. BES-II data analysis to obtain impulse spectra, check the self-similarity of particle production, estimate the constituent energy losses, study cumulative particle production and search for phase transition signatures.
2. The event-by-event analysis of Au + Au collisions at energies  $\sqrt{s_{NN}}=200$  GeV and different centralities obtained by STAR at RHIC, with the aim of searching for fractal structures. The further development of the method for fractal analysis of events of nucleus-nucleus interactions.
3. Participation in the Hot QCD Physics Program with emphasis on the study of pseudorapidity dependence of global hyperon polarisation (see subsection 4.1).
4. Participation in the Cold QCD Physics Program and study of spin effects in collisions of polarized protons with protons and nuclei (see subsection 4.2).

### ***Cold QCD Physics with $p\uparrow + p\uparrow$ Collisions at 510 GeV:***

- inclusive transverse spin asymmetries at forward rapidities;
- transversity, Collins function and interference fragmentation function;
- Sivers and Efremov-Teryaev-Qiu-Sterman function.



### ***Polarized $p\uparrow + p$ and $p\uparrow + A$ collisions at 200 GeV:***

- forward transverse spin asymmetries;
  - Sivers effect;
  - transversity and related quantities.
5. Analysis of data from fixed target experiments (see subsection 3.2):
- high moments of proton multiplicity distributions,
  - new results on hypernuclei production ( ${}^4_{\Lambda}\text{H}$ ,  ${}^5_{\Lambda}\text{He}$ ).
6. There is enhanced interest to the production of light ions, which surprisingly appears to be in agreement with predictions of particle number ratios in both statistical and coalescence models. The first model is unjustified due to a huge difference between the temperature of chemical freeze-out of  $\sim 160$  MeV and the binding energy of a few MeV. A possibility to distinguish these models has been suggested based on the yields of  ${}^4\text{Li}$  and  ${}^4\text{He}$ .
7. New BES-II net-proton kurtosis and light nuclei yield ratio measurements and their data analysis, including in particular measurement at minimal collider energy 7.7 GeV and additional measurement at 16.7 GeV.

## **5.1. Femtoscopy Correlation**

At the previous stages of the project, the JINR group made a great contribution to the study of femtosopic correlations. Among these results are:

- “The measurement of the  $\Lambda\Lambda$  interaction”, STAR Collab. Phys. Rev. Lett. 114, 022301 (2015);
- “Measurement of interaction between antiprotons”, STAR Collab. Nature 527 (2015) 345.

Also, new theoretical approaches have been developed for studying the space-time picture, the effects of the final state interactions and spin-spin correlations:

- “Spin correlations and consequences of quantum-mechanical coherence”, R. Lednicky and V. L. Lyuboshitz, Phys. Lett. B 508 (2001) 146;
- “Correlation femtoscopy of multiparticle processes”, R. Lednicky, Phys. of Atomic Nuclei 67 (2004) 71;
- “Femtoscopic search for the phase transition”, R. Lednicky, Nucl. Phys. B (Proc. Suppl.) 198 (2010) 43.

Below, it is proposed to use the femtosopic correlation method to analyze new experimental data obtained using the BES-II program at the collider and with a fixed target. It is planned to pay special attention to the energy interval close to the energy region expected in the NICA/MPD and BM@N experiments.

1. In high energy particle or nuclei collisions, large numbers of various particles are produced. Particle momentum correlations due to the effects of final state interaction (FSI) and quantum statistics (QS) at small relative momenta in their centre-of-mass system, as well as, – particle coalescence due to FSI, allow one to get space-time characteristics of the production processes on a femtometer level; at the same time, they provide the information on particle strong interaction hardly accessible by other means (see a review [1] and references therein).

2. Of particular importance is a systematic study of the production space-time parameters in the beam energy scan, together with the fluctuation characteristics, in the search for the critical endpoint and corresponding softening of the Equation of State (EoS) and increased duration of particle emission (see, e.g., [2,3]). Besides correlations of identical particles, providing information on even moments of the distribution of particle space-time separation, also the correlations of non-identical particles should be studied, the latter providing, in addition, also the information on the odd moments, including space and time shifts [1]. Obviously, correlations in various combinations of pions, kaons, nucleons and hyperons contain a rich complementary information about the production process.

3. The correlation measurement of strong particle interaction is especially up-to-date in connection with the so-called hyperon puzzle in neutron stars. Their radius of 10–15 km and mass of  $\sim 1.5$ – $2$  sun masses essentially depend on the EoS, which is softened in the presence of hyperons thus leading to a decrease of the maximal neutron star mass [4]. Unfortunately, the present knowledge of hyperon-nucleon, hyperon-hyperon, kaon-nucleon and kaon-hyperon interactions is not sufficient for a reliable calculation of nucleon and hyperon fractions and corresponding neutron star EoS.

4. The measurement of the  $\Lambda\Lambda$  interaction is of particular interest in connection with a possible existence of so-called H-dibaryon. The STAR analysis of  $\Lambda\Lambda$  correlations in Au + Au collisions reported a negative singlet s-wave scattering length  $f_0 \approx -1$  fm (defined as the scattering amplitude at threshold) and a large positive effective radius  $d_0 \approx 8$  fm thus excluding both a near threshold s-wave resonance and a  $\Lambda\Lambda$  bound state (the latter requiring [6]  $2d_0/f_0 > -1$ , i.e.,  $d_0 < 0.5$  fm). On the contrary, a recent ALICE analysis of  $\Lambda\Lambda$  correlations in  $p + p$  and  $p + \text{Pb}$  collisions is compatible with the existence of a  $\Lambda\Lambda$  bound state [7]. This discrepancy calls for a new analysis of STAR data with higher statistics and a more refined treatment of residual correlations due to feed-down  $\Lambda$ 's from hyperon decays (dominantly, from  $\Sigma^0 \rightarrow \Lambda\gamma$ ).

5. Another possibility to extract the  $\Lambda\Lambda$  singlet scattering parameters is the analysis of  $\Lambda$  spin correlations using as a spin analyser the asymmetric (parity violating) decay  $\Lambda \rightarrow p\pi^-$ : the distribution of the cosine of the relative angle  $\theta$  between the directions of the decay protons in the respective  $\Lambda$  rest frames allows one to determine the triplet fraction of the  $\Lambda\Lambda$  correlation function [8]. Since this technique requires no construction of the uncorrelated reference sample, it can serve as an important consistency check of the standard correlation measurements. This technique can be especially useful for the analysis of  $\Lambda\Lambda$  correlations in  $p + p$  or  $p + \text{A}$  collisions, where the characteristic Gaussian source radius  $r_0$  is rather small ( $\sim 1$ – $1.5$  fm) and the correlation width  $1/r_0 \sim 200$  MeV/ $c$  is sufficiently large for a statistically significant analysis.

6. The two-particle FSI in multiparticle production processes is usually taken into account in a similar way as in beta-decay by substituting the product of plane waves at equal times in pair rest frame (PRF) with the two-particle wave function of the corresponding scattering problem. Obviously, this assumption is not justified at very large temporal particle separation  $t^*$  in PRF, when the two-particle FSI should vanish. On the other hand, it was shown [9,10] that one can neglect the  $t^*$  separation on conditions  $|t^*| \ll m(t^*)r^* \text{Min}(r^*, 1/k^*)$ , where  $m(t^* > 0) = m_2$ ,  $m(t^* < 0) = m_1$ ;  $r^*$  and  $k^*$  are spatial particle separation and particle momentum in PRF. These conditions are presumably well satisfied for correlations between heavy particles like kaons or protons, but their violation for correlations involving pions is not excluded (expectedly, on a level of several percent). The former statement was confirmed by the STAR correlation measurement of the

proton-proton and antiproton-antiproton scattering parameters in perfect agreement with their table values [11]. As for the correlations involving pions, the validity check of the equal-time ( $t = 0$ ) approximation still remains to be done. An attempt of this check was done using the NA49  $\pi^+\pi^-$  correlation data, pointing to  $\sim 20\%$  underestimation of the  $s$ -wave  $\pi^+\pi^-$  scattering length, however, with the statistical significance of two standard deviations only [1].

## 5.2. Monte Carlo simulation and software development

### ▪ *Event-by-event Monte Carlo simulation and comparison with STAR data*

It is planned to study the structure of Au + Au events obtained by the Monte Carlo method using the A Multiparticle Transport Model (AMPT) generator at a collision energy  $\sqrt{s_{NN}} = 200$  GeV and different centralities.

The search for new physical laws, as a rule, relies on a comparison of the results of the analysis of experimental data with the available results of theoretical calculations. The detected difference is considered as an indication of the effects not considered in the model description and contributes to a more complete development of theoretical models and approaches.

The AMPT generator is widely used by both STAR and other collaborations to simulate ion interaction events depending on the energy, impact parameter of the collision, and to obtain different distributions of produced particles.

The JINR group plans to carry out an event-by-event analysis of Au + Au collisions at energies  $\sqrt{s_{NN}} = 200$  GeV and different centralities obtained using the AMPT generator in order to find the difference in distributions in fractal dimensions. It is assumed that such a sophisticated analysis will contribute to a deeper understanding of the mechanisms inherent in the model and the degree of their correspondence to the experimentally studied physical processes.

It is planned to compare the results of fractal analysis of events obtained by STAR at the RHIC and the Monte Carlo method to search for the peculiarities of the properties of nuclear matter formed in collisions of heavy ions.

### ▪ *Development of particle identification*

In 2019 and 2020, the STAR collaboration carried out a major upgrade of the installation, including TPC, and collected a large amount of data under the BES II program. Since the increase in the number of points on the track and the new algorithm for calculating the energy losses of particles in the TPC gas significantly changed the detector's response function to different types of charged particles, it became necessary to obtain a new approximation of this function. A significant increase in data statistics and an increase in the efficiency of the software for searching for neutral particles makes it possible to form a new, much cleaner set of particles for determining the TPC response function to protons, pions, kaons and electrons. To do this, using the KFParticle algorithm, the distribution of energy losses of different types of particles depending on their momentum and centrality of interaction was obtained from the data processed during the collection of collisions of gold nuclei at different energies. Now, a search is underway for a mathematical function or a set of functions that will allow describing the obtained dependencies with an accuracy better than 2%. Further, these descriptions of the response functions are planned to be applied to determine the magnitude of fluctuations of the moments of the distribution of the multiplicity of particles in collisions of gold nuclei, depending on their centrality and energy.

- ***Turning on the event plane detector into data analysis***

The work related to the inclusion of an event plane detector (EPD) in the complex of programs for processing data has been carried out. The event plane detector will increase the accuracy of event reconstruction in experiments to study global polarization and measure directed flows and other collective effects in nucleus-nucleus collisions. The results of the runs in which the event plane detector worked in the STAR experiment at RHIC since its launch in 2018 are analyzed. The software for launching the systems of codes “Event Plane with the STAR EPD code StEpdEpFinder” is installed. Within the framework of StEpdEpFinder, the data on collisions of Au + Au nuclei at energy  $\sqrt{s_{NN}} = 27$  GeV in the STAR experiment at RHIC, taking into account information from the event plane detector, have been processed. Using StEpdEpFinder, information was obtained on the plane of the event in collisions of gold nuclei at energies  $\sqrt{s_{NN}} = 27$  GeV. The estimation of the value of the direct flow ( $v_1$ ) for Au + Au collisions at an energy  $\sqrt{s_{NN}} = 27$  GeV was also obtained. The analysis results indicate the presence of a nonzero value of  $v_1$ .

In the MpdRoot repository, the algorithm developed by the MPD thread group has been tested and the necessary functions have been selected to determine the angle of the plane of the event using the ZDC (hadron calorimeter for high rapidities). Knowing the energy release in each cell of the hadron calorimeter for high rapidity, it is possible to reconstruct the angle of the plane of the event from the forward flow. The resolution of the event plane can be calculated from the forward flow in the ZDC.

It is planned to transfer the tested and existing polarization algorithms to the online repository. The site github.com was chosen, which is positioned as a web service for hosting projects using the git version control system, as well as a social network for developers.

- ***Machine learning techniques to data analysis***

Given the experience with machine learning, it is planned to develop a convolutional neural network to find objects of interest in the image. It is planned to explore the possibility of machine learning in high energy physics, namely, the identification of charged particles based on machine learning. Particle identification based on trajectory geometry and TOF data analysis using a neural network. The characteristics used for identification are the particle momentum-to-charge ratio and mass-to-charge ratio, which we extract from the particle’s passage through detector data, modeled using the MpdRoot software package. The parameters of the particle momentum-to-charge ratio and the mass-to-charge ratio are fed to the input layer; the output layer consists of six softmax elements, which correspond to the probabilities of identifying a particle as one of six types. For machine learning, we plan to use the open software library TensorFlow. Now there is a process of studying the literature, discussing and developing a neural network.

Given the experience with machine learning, it is planned to develop a convolutional neural network to find objects of interest in the image. It is planned to explore the possibility of machine learning in high energy physics, namely, the identification of charged particles based on machine learning. Particle identification based on trajectory geometry and TOF data analysis using a neural network. The characteristics used for identification are the particle momentum-to-charge ratio and mass-to-charge ratio, which we extract from the particle's passage through detector data, modeled using the MpdRoot software package. The parameters of the particle momentum-to-charge ratio and the mass-to-charge ratio are fed to the input layer; the output layer consists of six softmax elements, which correspond to the probabilities of identifying a particle as one of six types. For

machine learning, we plan to use the open software library TensorFlow. Now there is a process of studying the literature, discussing, and developing a neural network.

### 5.3. Software infrastructure for the STAR data processing at JINR

- **STAR-JINR end-to-end GRID production**

The large luminosity of RHIC and high-speed data acquisition system at the STAR is allowed to collect more than 50 Petabytes of information about Au + Au collisions. And the amount of information increases every year. STAR’s RHIC computing facility provides over 15K dedicated slots for data reconstruction. This number of slots is not always sufficient to satisfy an ambitious and data-challenging physics program and harvesting resources from outside facilities are paramount to scientific success. However, constraints of remote sites (e.g. CPU time limits) do not always provide the flexibility of a dedicated farm. STAR has a breadth of smaller data sets (both in runtime and size) that can be easily offloaded to remote facilities with many such limits. Scavenged resources can be run with efficiency comparable to that of the local production and contributes additional computing time to an experiment that runs every year and therefore needs fast turnaround.

Therefore, the use of the distributed data centers of different institutions of the STAR collaboration is one of the possible solutions to this problem. The Laboratory of Information Technologies of the JINR became the world’s leading centers for the processing by the GRID system. Therefore, JINR resources can be used to process the STAR data. The JINR software group together with the STAR software group developed software stack of GRID production framework including dealing with multi-site submission, automated re-submission, job tracking, as well as new challenges and possible improvements. Technical solutions for the architecture of the GRID Software Stack and the organization of GRID Production Dataflow are shown in the two figures below.

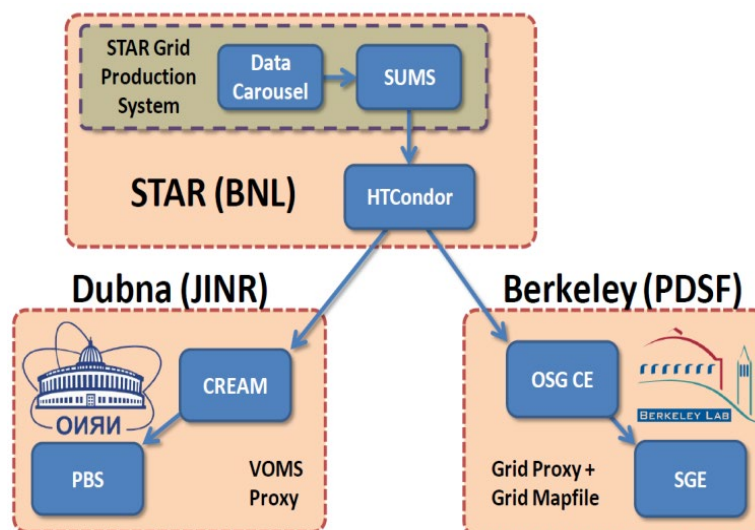


Figure 27. GRID Software Stack Architecture.

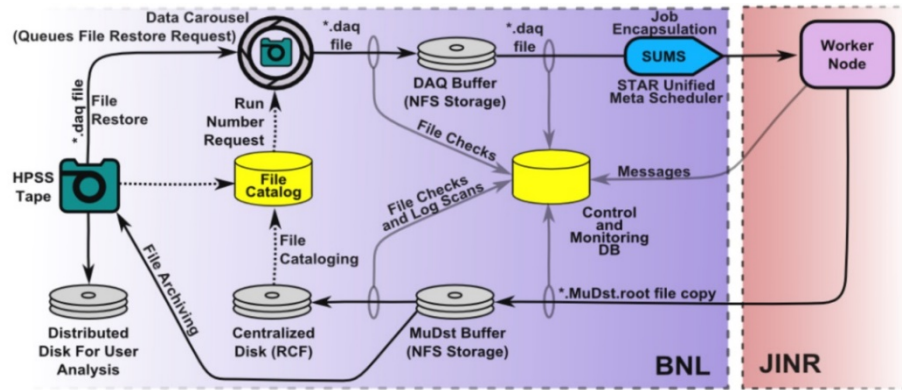


Figure 28. Current GRID Production Dataflow.

Our framework has an excellent first pass efficiency of 93.2 %. The efficiency is comparable to, but slightly lower than, local efficiency, which is 98 %, due to the additional complexity of the added software interfaces. STAR has put a lot of thought and iterative refinement into the design of this production system. Extensive preproduction testing and a well-structured finite state system applied to each job, with retries in the event of interruption, applied to each job contributes to this high efficiency. What makes this even more remarkable is that it is running on heterogeneous nodes.

#### ▪ *From MuDst to PicoDst format*

STAR is interested in developing newer and more compact analysis data format. The Data Summary file format known as a “MuDST” (micro-DST) was complemented by an emerging format known as “PicoDST”. The PicoDST related code workflows were since integrated in the STAR framework after a successful software peer-review process verifying code compliance. The Physics Working Group (PWG) conveners were actively polled for readiness and adaptation of ongoing analysis to the new file format and the PicoDST was extended for a wider acceptance across all physics topics.

The generation of PicoDST from Micro-DST is a recent process by which, a more compact (and newly introduced) format could be produced from past data. The jobs are short, possibly a good match for the queue limitations at Dubna and pending a test on how many transfers we can sustain with the current infrastructure, we aim at directing the whole PicoDST production at the JINR/Dubna site. Currently, over a million files production was requested from the PWG. We did this work on converting MuDst to PicoDst at JINR in 2019–2020. We would like to emphasize that the PicoDST format is very convenient for the goals of the Dubna group. It allows to install STAR software libraries and gives possibility to analyze STAR data at modern personal computers without direct communication with RHIC computer facilities.

## 6. References

1. R. Lednicky, Phys. of Atomic Nuclei 67 (2004) 71.
2. R. Lednicky, Nucl. Phys. B (Proc. Suppl.) 198 (2010) 43.
3. P. Batyuk et al., Phys. Rev. C 96 (2017) 024911.
4. D. Lonardonni et al., Phys. Rev. Lett. 114 (2015) 092301.
5. STAR Collab. (L. Adamczyk et al.), Phys. Rev. Lett. 114 (2015) 022301.
6. P. Naidon and S. Endo, Rept. Prog. Phys. 80 (2017) 056001.

7. ALICE Collab. (S. Acharya et al.), *Phys. Lett. B* 797 (2019) 134822.
8. R. Lednicky and V. L. Lyuboshitz, *Phys. Lett. B* 508 (2001) 146.
9. R. Lednicky and V.L. Lyuboshitz, *Sov. J. Nucl. Phys.* 35 (1982) 770.
10. R. Lednicky, *Phys. Part. Nuclei* 40 (2009) 307.
11. STAR Collab. (L. Adamczyk et al.), *Nature* 527 (2015) 345.
12. S. Bazak and St. Mrowczynski, *Eur. Phys. J. A* 56 (2020) 193.



# Appendix 1. Form No. 26

Form No. 26

## Schedule proposal and resources required for the implementation of the Project

### STAR (JINR participation)

(Project title)

| Expenditures, resources, financing sources |   | Costs (k\$)<br>Resource requirements  | Proposals of the Laboratory on the distribution of finances and resources |           |           |
|--|---|---|---|-----------|-----------|
|  |   |   | 2022  | 2023      | 2024      |
| Expenditures                               | Main units of equipment, work towards its upgrade, adjustment etc.  | 60  | 20  | 20        | 20        |
|  | Materials   | 15  | 5   | 5         | 5         |
| Required resources                         | Standard hour   |   |   |           |           |
|  | Resources of<br>– Laboratory design bureau;<br>– JINR Experimental Workshop;<br>– Laboratory experimental facilities division;<br>– accelerator;<br>– computer.<br>Operating costs. |   |   |           |           |
|  | Payments for agreement-based research   | 45  | 15  | 15        | 15        |
| ISTC                                       | Travel allowance, including:<br>a) Non-rouble zone countries<br>b) rouble zone countries<br>c) protocol-based   | 165   | 55  | 55        | 55        |
| Financing sources                          | Budgetary resources   | <b>285</b>  | <b>95</b>   | <b>95</b> | <b>95</b> |
|  | External resources  | Contributions by collaborators.<br>Grants.<br>Contributions by sponsors.<br>Contracts.<br>Other financial resources, etc. |   |           |           |

PROJECT LEADER

*Handwritten Signature*  
SIGNATURE

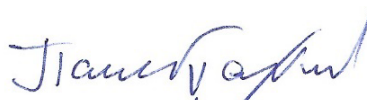
## Estimated expenditures for the Project STAR (JINR participation)

Investigation of the properties of nuclear matter and particle structure at the collider of relativistic nuclei and polarized protons

(full title of Project)

| Expenditure items                        | Full cost  | 2022      | 2023      | 2024      |
|--|------------|-----------|-----------|-----------|
| Direct expenses for the Project          |            |           |           |           |
| 1. Accelerator, reactor                  | –          | –         | –         | –         |
| 2. Computers                             | –          | –         | –         | –         |
| 3. Computer connection                   | –          | –         | –         | –         |
| 4. Design bureau                         | –          | –         | –         | –         |
| 5. Experimental Workshop                 | –          | –         | –         | –         |
| 6. Materials                             | 15         | 5         | 5         | 5         |
| 7. Equipment                             | 60         | 20        | 20        | 20        |
| 8. Construction/repair of premises       | –          | –         | –         | –         |
| 9. Payments for agreement-based research | 45         | 15        | 15        | 15        |
| 10. Travel allowance, including:         | 165        | 55        | 55        | 55        |
| a) non-rouble zone countries             |            |           |           |           |
| b) rouble zone countries                 |            |           |           |           |
| c) protocol-based                        |            |           |           |           |
| <b>Total direct expenses</b>             | <b>285</b> | <b>95</b> | <b>95</b> | <b>95</b> |

PROJECT LEADER



LABORATORY DIRECTOR



LABORATORY CHIEF ENGINEER-ECONOMIST



### Appendix 3. List of conference reports

Список публикаций с существенным вкладом группы ОИЯИ приведен непосредственно в каждом разделе текста extended annotation. Здесь мы приводим список докладов членов Дубненской группы at international conferences, meetings of the STAR collaboration and seminars:

A list of publications with significant contribution of the JINR group is given directly in each section of the extended annotation text. Here we provide a list of reports of members of the Dubna group at international conferences, meetings of the STAR collaboration and seminars:

1. “z-Scaling from hundreds of MeV to TeV”, Relativistic Nuclear Physics from hundreds of MeV to TeV”, May 26–June 1, 2019, StaraLesna, Slovakia.
2. “High- $p_T$  spectra of h-hadrons in Au + Au collision at  $\sqrt{s_{NN}} = 9.2$  GeV”, STAR Collaboration Meeting, 14–25 September, 2020, Indian Institute of Science Education and Research (IISER) Tirupati, India.
3. “Search for fractal structures in Au + Au events at 200 GeV”, STAR Collaboration Meeting, 14–25 September, 2020, Indian Institute of Science Education and Research (IISER) Tirupati, India.
4. “Self-similarity, fractality and entropy principle in collisions of hadrons and nuclei at RHIC, Tevatron and LHC”, 40th International Conference on High Energy physics – ICHEP2020, July 28 – August 6, 2020, Prague, Czech Republic.
5. “Self-similarity of the proton spin”, Workshop “Physics programme for the first stage of the NICA SPD experiment”, JINR, Dubna, LHEP, 5–6 October 2020.
6. «Методика восстановления лямбда гиперонов в ядро-ядерных столкновениях», Семинар в Национальном Центре Ядерных Исследований, г. Баку 21.01.2020
7. “STAR Recent Results on Heavy-Ion Collisions”, LXX International Conference NUCLEUS-2020, online conference, 11–17 October 2020.
8. “Investigation of the beam energy dependence of particle production in gold collisions at MPD energy region”, XXIV International Scientific Conference of Young Scientists and Specialists (AYSS-2020), online conference, 9–13 November 2020.